Härtl, Tilmann

Conference Paper

Identifying Proxy VARs with Restrictions on the Forecast Error Variance

Beiträge zur Jahrestagung des Vereins für Socialpolitik 2022: Big Data in Economics

Provided in Cooperation with:
Verein für Socialpolitik / German Economic Association

Suggested Citation: Härtl, Tilmann (2022) : Identifying Proxy VARs with Restrictions on the Forecast Error Variance, Beiträge zur Jahrestagung des Vereins für Socialpolitik 2022: Big Data in Economics, ZBW - Leibniz Information Centre for Economics, Kiel, Hamburg

This Version is available at:
https://hdl.handle.net/10419/264071

Identifying Proxy VARs with Restrictions on the Forecast Error Variance

Tilmann Härtl

Department of Economics, University of Konstanz

tilmann.haertl@uni-konstanz.de

*

February 14, 2022

Abstract

The proxy VAR framework requires additional restrictions to disentangle the structural shocks when multiple shocks are identified using multiple instruments. I propose to employ restrictions on the forecast error variance (FEV). Less restrictive assumptions that bound the contributions to the FEV can replace or accompany inequality restrictions on e.g. the impulse responses. This enables or sharpens the set identification of the structural parameters. Furthermore, with the correct economic intuition the Max-Share framework can be used to point identify the structural parameters without the need for strict equality restrictions in the case when two shocks are identified with two proxy variables.

*German Science Foundation (DFG) grant number BR 2941/3-1 is gratefully acknowledged.

1 Introduction

In the last decade, proxy variables were highly prevalent in the structural vector autoregression (SVAR) literature. The proxy VAR framework was developed by Stock and Watson (2012) and Mertens and Ravn (2013). So far, it was applied to identify the effects of various structural shocks. For example, Mertens and Ravn (2013) estimate the effects of taxation shocks, Gertler and Karadi (2015) the effects of monetary policy shocks and Piffer and Podstawski (2018) the impacts of uncertainty shocks. As in the standard IV identification the proxy variables (also called instruments in this context) need to satisfy two key conditions. Reminiscent of the relevance and exogeneity assumption, the external series have to be related to the target shocks of interest while being unrelated to the remaining structural shocks that are not identified.

When multiple shocks are identified with multiple instruments, Mertens and Ravn (2013) show that additional identifying restrictions are needed in order to disentangle the structural shocks. For instance, Piffer and Podstawski (2018) have an instrument related to an uncertainty shock and one instrument for a news shock. If the two instruments are not related to structural shocks other than the uncertainty and news shock, the proxy VAR successfully rules out the other shocks as confounders. Yet, in order to disentangle the two identified shocks additional restrictions are needed. Different solution were proposed in the literature. Mertens and Ravn (2013) assume a recursive structure, meaning that one of their two identified shocks has no contemporaneous impact on a specified variable. Piffer and Podstawski (2018) distinguish between uncertainty and news shocks by enforcing that each shock is correlated more strongly to the instrument targeting it.

For the latter strategy, the inequality restriction results in the set identification of the structural parameters. Yet, the set identification strategies inherit the potential to lead to rather large and uninformative sets if the identification restrictions are not sharp enough. On the contrary hard equality restrictions which sharply identify the structural parameters, as e.g. in Mertens and Ravn (2013), are typically hard to defend. The difficulties in both cases highlight the importance of economic intuition in the identification of SVARs. I propose to use restrictions on the contribution of a specific shock to the forecast error variance (FEV) of a target variable in order to disentangle the identified shocks in the proxy VAR. Depending on the available economic intuition the FEV restrictions allows both point and set identification.

Set identification of shocks based on restrictions on the contributions to the FEV were introduced by Volpicella (2021). The main idea is to bound the contributions of the target shock to the FEV of a specified variable. These bounds induce inequality restrictions on the structural model, similar to e.g. sign restrictions, and the identi-

fied set consists of all the structural representations that satisfy them. The bounds on the FEV can either replace or accompany existing inequality restrictions. Hence, the bounds offer a possibility to identify the impulse responses, which are often the key element of interest in the SVAR environment, without the need to impose restrictions on exactly the parameters of interest. Yet, if the bounds on the FEV accompany existing inequality restrictions they help to sharpen the identification and alleviate the problem of large uninformative identified sets.

Point identification of shocks via restrictions on the FEV dates back to Faust (1998) and Uhlig (2004a) and was originally an alternative to the bias prone long-run restrictions. The shock is identified to be the shock that maximizes the contribution to the FEV of a specific variable. Francis et al. (2014) coined the term 'Max-Share' for this identification strategy and in the following I use this expression to refer to it. However, Dieppe et al. (2019) point out the as soon as more than one shock contributes to the FEV of the chosen variable, the maximization of the share identifies a combination of the contributing shocks. Due to this drawback the Max-Share approach is only in specific situations applicable. In the literature it has, for instance, been used by Barsky and Sims (2011) to identify technology news shocks and by Ben Zeev and Pappa (2017) to identify defence spending news shocks.

The merit of fusing proxy VARs and the Max-Share approach is that sharp point identification of the structural parameters is achieved without the need for strict equality restrictions. Certainly, the drawback of the pure Max-Share framework carries over to the application in the proxy VARs. Hence, the Max-Share approach only correctly disentangles the underlying shocks if one of them exclusively contributes to a variable in the system. Shocks that contribute to the FEV but are not related to the proxies are cancelled out by the proxy VAR. Yet, if the condition of exclusive contribution is not fulfilled the results will be biased. Thus, I propose to augment the Max-Share framework with an inequality restriction to disentangle the shocks while removing or reducing the bias. This strategy is limited to the case when two shocks are identified with two instruments. However, in practice this highly relevant as finding two suitable proxy variables is difficult enough. The inequality restriction is of the form that the contemporaneous impact of shock one on a specified variable is larger than the impact of shock two on the same variable. If known, one can also incorporate the margin by which the response to the one shock exceeds the response of the other shock into the inequality constraint to reduce the bias further.

The simulation study shows that the Max-Share approach successfully disentangles the shocks in the proxy VAR. In the case of exclusive contributions the basic Max-Share identification is sufficient to disentangle the structural shocks. If the basic Max-Share framework is biased the augmentation with the mentioned inequality

constraint reduces or removes the bias depending on the specification of the additional constraint. The closer the inequality constraint to the actual margin of the restricted contemporaneous responses the closer the estimate to the true underlying structural parameters.

Compared to the Max-Share framework the bounds offer a more flexible approach with less restrictive assumptions and it can be easily combined with other types of restrictions. Yet, the benefits come with the cost of loosing the sharp point identification. Nevertheless, bounding the FEV is a useful identification strategy whose assumptions can be backed with economic theory and intuition. I present an empirical illustration which highlights one useful application of the bound constraints. I weaken the strict identification assumption by Mertens and Ravn (2013) and show that their results are, although qualitatively not considerably different, statistically less convincing.

Section two commences with the introduction of the baseline SVAR framework and the introduction of the proxy VAR. Section three describes the usage of restrictions on the FEV for the identification of the structural VAR. It starts with the more general set identification approach via the bounds on the FEV and ends with the more strict point identification via the Max-Share framework. Section four and five present the results of the simulation study and of the empirical illustration, respectively.

2 Econometric Framework

2.1 The Structural VAR

The starting point is the k dimensional stationary structural VAR(p) model:

$$y_t = \sum_{m=0}^{p} A_m y_{t-l} + Bw_t, \quad t = 1, ...T, \tag{1}$$

where the $k \times 1$ vector w_t depicts the economically meaningful structural shocks (e.g. Kilian & Lütkepohl, 2017). The $k \times k$ impact matrix B maps the reduced form innovations into the structural shock, $u_t = Bw_t$. The elements of the $k \times 1$ white noise vector u_t are the reduced form innovations. To shorten the notation one can rewrite the SVAR in (1) as:

$$y_t = Ax_t + Bw_t, \quad t = 1, ...T, \tag{2}$$

with $x_t = (y'_{t-1}, ..., y'_{t-p})'$ and $A = (A_1, ..., A_p)$. A constant is omitted for the brevity of the notation but it can be included in a straightforward way.

Common to most identification strategies is the normalization $\mathbb{E}(w_t w_t') \equiv \Sigma_w = I_K$, which yields the set of covariance restriction $\mathbb{E}(u_t u_t') \equiv \Sigma = BB'$. Without further assumptions these restrictions do not suffice to pin down the structural parameters as the resulting system of equation has many possible solutions. The Cholesky decomposition of Σ, denoted by Σ_c, satisfies these covariance restrictions. Yet, they will also hold for every rotation with an $k \times k$ orthonormal matrix Q, $\Sigma = \Sigma_c \Sigma_c' = \Sigma_c Q Q' \Sigma_c'$. Giacomini, Kitagawa, and Read (2021) refer to this representation of the SVAR as the 'orthogonal reduced form'.

The moving average representation of the SVAR is then given by:

$$y_t = \sum_{m=0}^{\infty} C_m \Sigma_c Q w_{t-m}, \quad t = 1, ...T, \tag{3}$$

where the $k \times k$ matrices C_m contain the moving average coefficients which give the response of the system to the reduced form innovations m periods ago. The impulse response of variable i to shock j at horizon h is given by:

$$\eta_{i,j,h} = e_i' C_m \Sigma_c q_j, \tag{4}$$

where e_i and e_j are the ith and jth column of I_k, respectively, and q_j is the jth column of Q.

Apart from the impulse response functions the FEV decomposition is are an element of interest in the SVARs. In this paper the FEV decomposition is particularly of importance as identifying restrictions are placed on it. To formalize the FEV decomposition let the h-step-ahead forecast of y_t be:

$$y_{t+h|t} = \sum_{m=0}^{\infty} C_{h-m} u_{t-m}. \tag{5}$$

The h-step ahead forecast error is then given by:

$$y_{t+h} - y_{t+h|t} = \sum_{m=0}^{h-1} C_m \Sigma_c Q w_{t+h-m}, \tag{6}$$

and the h-step ahead forecast error covariance matrix is represented by:

$$\Omega(h) = \sum_{m=0}^{h-1} C_m \Sigma_c Q Q' \Sigma_c' C_m' = \sum_{m=0}^{h-1} C_m \Sigma C_m'. \tag{7}$$

The contribution from shock j to the total forecast variance of variable i at horizon

h is then:

$$\Omega_{i,j}(h) = \frac{e_i'(\sum_{m=0}^{h-1} C_m \Sigma_c q_j q_j' \Sigma_c' C_m')e_i}{e_i'(\sum_{m=0}^{h-1} C_m \Sigma C_m')e_i}, \tag{8}$$

where e_i is the ith column of the identity matrix I_k and q_j is the jth column of Q.

In order to identify the structural parameters of interest restrictions have to be placed on the model. As mentioned before two different identification schemes exist. Set identification amounts to finding all the rotation matrices Q that satisfy the identification restrictions. In turn, they define the identified set for e.g. the impulse response functions or the FEV decomposition. Common set identification restrictions are, for instance, inequality restriction on the structural impulse responses. The stricter the identifying restrictions, the smaller the identified set. In point identification schemes the restrictions are such that only one admissible rotation matrix Q exists. The typical point identification restrictions are equality restrictions on the elements of the impact matrix B. For example, $k(k-1)/2$ independent equality restrictions on B are sufficient to point identify the structural parameters.

The proxy VAR framework that is introduced in the next subsection allows both for point and set identification. If one shock is identified using one proxy variable the parameters are point identified up to scale. With multiple shocks and multiple proxies additional restrictions are needed in order to disentangle the shocks. In the latter case the just mentioned sign or equality restrictions are one possibility and depending on the type of imposed restrictions the structural parameters are either point or set identified.

2.2 Proxy VAR

For the the proxy VAR framework I loosely follow the framework by Giacomini et al. (2021) as the inference for the set identification part will be based on their work. As in the standard instrumental variable (IV) framework, the proxy variables - also called instruments interchangeably - have to satisfy two key assumptions. Without loss of generality, let z_t be a $l \times 1$ vector of instruments that are related to the first l structural shocks in w_t. The two following two conditions have to be satisfied:

$$\mathbb{E}(z_t w_{(1:l),t}) = \Psi \quad \text{and} \quad \mathbb{E}(z_t w_{(k-l+1:k),t}) = 0, \tag{9}$$

where Ψ is an $l \times l$ matrix of full rank. These two conditions resemble the relevance and exogeneity conditions of the standard IV approach. The instruments have to be related to the target shocks and unrelated to the remaining structural shocks.

Assume that the proxies follow:

$$\Gamma_0 z_t = \Lambda w_t + \sum_{l=0}^{p_m} \Gamma_m z_{t-l} + \nu_t, \quad t = 1, ..., T. \tag{10}$$

The process in (10) indicates that the proxies are related to the structural shocks. Giacomini et al. (2021) assume that $(w_t', \nu_t)' | \mathcal{F}_{t-1} \sim N(0_{(k+l)\times l}, I_{k+l})$, where $\mathcal{F}_{t-1}$ is the information set at time $t-1$.

The assumptions in (9) together with process (10) yield:

$$\mathbb{E}(z_t w_t') = \Gamma_0^{-1}\Lambda = [\Psi, 0_{l\times(k-l)}]. \tag{11}$$

Plugging model (2) into the process in (10) and left-multiplying by Γ_0^{-1} yields:

$$z_t = Dy_t + Gx_t + \sum_{m=0}^{p_z} H_m z_{t-m} + v_t, \quad t = 1, ..., T, \tag{12}$$

where $D = \Gamma_0^{-1}\Lambda B^{-1}, G = -\Gamma_0^{-1}\Lambda A$ and $H_m = \Gamma_0^{-1}\Gamma_l$ for each $m = 1, ..., p_z$.

Giacomini et al. (2021) show that (11) can also be represented by:

$$\mathbb{E}(z_t w_t') = D\Sigma_c Q = [\Psi, 0_{l\times(k-l)}], \tag{13}$$

implying that the relevance assumption $\text{rank}(\Psi) = l$ is fulfilled if and only if $\text{rank}(D) = l$. The exogeneity and relevance assumption regarding the proxies restricts the rotation matrices Q such that they follow the structure in (13). In this fashion the proxy VAR shrinks the identified set.

In the following I deviate from the notation of Giacomini et al. (2021) and use the proxy VAR framework by Piffer and Podstawski (2018). This allows me to handle both the bounds on the FEVD and the combination with Max-Share approach in the same proxy VAR framework. The next section describes how the robust bayesian inference algorithm of Giacomini et al. (2021) is adapted to the representation of the proxy SVAR below.

Following Piffer and Podstawski (2018), I decompose the reduced form errors into two components:

$$u_t = B_z w_{(1:l),t} + B_{-z} w_{(k-l+1:k),t}, \quad t = 1, ..., T, \tag{14}$$

where B_z is the $k \times l$ block of the impact matrix B that contains the first l colums and B_{-z} is the according remaining part of B. B_z contains the structural parameters of the shocks related to the proxies whose identification is the goal of the proxy VAR. I refer to this matrix as the 'proxy impact matrix'. Considering (14) together with

the assumption regarding the proxies in (9) yields $\mathbb{E}(u_t z_t') = B_z \Psi' = Z$. Equation (13) lets me rewrite this expected value:

$$\mathbb{E}(u_t z_t') = B\mathbb{E}(w_t z_t') = B\mathbb{E}(z_t w_t')' = \Sigma D', \tag{15}$$

with $B = \Sigma_c Q$ and $\mathbb{E}(z_t w_t') = D\Sigma_c Q$. Hence, $\Sigma D' = Z = B_z \Psi'$. Partitioning the matrix $\Sigma D'$ and B_z yields:

$$\Sigma D' = Z = \begin{pmatrix} Z_1 \\ Z_2 \end{pmatrix} \; and \;\; B_z = \begin{pmatrix} B_{11} \\ B_{21} \end{pmatrix} \tag{16}$$

and thus

$$B_{21} = Z_2 Z_1^{-1} B_{11} = Z_l B_{11}, \tag{17}$$

where Z_1 is the upper $l \times l$ block of the matrix Z and B_{11} is the upper $l \times l$ block of B_z. Hence,

$$B_z = \begin{pmatrix} B_{11} \\ Z_l B_{11} \end{pmatrix}, \tag{18}$$

and if the upper $l \times l$ block B_{11} is identified the remaining block of the proxy impact matrix is identified as well. In order to identify the upper block of B_z decompose the matrices of the standard covariance restrictions $\mathbb{E}(u_t u_t') \equiv \Sigma = BB'$ such that:

$$\begin{pmatrix} \Sigma_{11} & \Sigma_{12} \\ \Sigma_{21} & \Sigma_{22} \end{pmatrix} = \begin{pmatrix} B_{11} & B_{12} \\ B_{21} & B_{22} \end{pmatrix} \begin{pmatrix} B_{11} & B_{21} \\ B_{12} & B_{22} \end{pmatrix}, \tag{19}$$

where Σ_{11} is the upper left $l \times l$ block of Σ. B_{11} is again the upper $l \times l$ block of B^z and therefore the upper left block of B. The remaining blocks of the two matrices have the according dimensions. It can be shown that $B_{11}B_{11}' = \Sigma_{11} - B_{12}B_{12}'$ (see Piffer & Podstawski, 2018) with:

$$B_{12}B_{12}' = (\Sigma_{21} - Z\Sigma_{11})'\Pi^{-1}(\Sigma_{21} - Z\Sigma_{11}), \tag{20}$$

$$\Pi = \Sigma_{22} + Z'\Sigma_{11}Z' - \Sigma_{21}Z' - Z\Sigma_{21}'. \tag{21}$$

Similar to the covariance restrictions $\mathbb{E}(u_t u_t') \equiv \Sigma = BB'$, the equation $B_{11} = \Sigma_{11} - B_{12}B_{12}'$ does not pin down the parameters of B_{11} uniquely. Let B_{11}^c be the Cholesky decomposition of $\Sigma_{11} - B_{12}B_{12}'$, then every rotation of B_{11}^c with an $l \times l$ orthonormal matrix Q will also satisfy $B_{11} = B_{11}^c B_{11}^{c'} = B_{11}^c QQ' B_{11}^{c'} = \Sigma_{11} - B_{12}B_{12}'$.

The exogeneity and relevance restriction regarding the proxies is satisfied for B_z by construction. Hence, the identification boils down to finding the set of $l \times l$ orthonormal matrices Q that satisfy the additional identifying restrictions, e.g. inequality restriction on structural parameters. In the next section I describe how

inequality restrictions on the FEV like in Volpicella (2021) fit into this framework.

It is also possible to point identify the structural parameters, what again comes down to finding the one rotation matrix for which the restrictions are satisfied. If the resulting recursive structure of B_{11}^c for the contemporaneous impacts of the identified shocks is economically justifiable, the Cholesky decomposition immediately point identifies the structural shocks. This is, for instance, the identification assumption used in Mertens and Ravn (2013) and the corresponding rotation matrix is just $Q = I_l$.

A special case arises when $l = 2$, meaning that two shocks are identified with two instrument. In the proxy VAR the rotation matrix will be of dimension 2×2. In this case, knowing one column of the rotation matrix also gives the second column of the rotation matrix Q up to a sign normalization. If the first column of a 2×2 orthogonal matrix is known the second column is pinned down up to sign through following equations:

$$Q = \begin{pmatrix} q_{11} & q_{12} \\ q_{21} & q_{22} \end{pmatrix}, \qquad 1 = q_{21}^2 + q_{22}^2 \quad \text{and} \quad 1 = q_{11}^2 + q_{12}^2.$$

Hence, restrictions on one of the two shocks are sufficient to identify both shocks of interest. The second shock is pinned down due to the properties of orthogonal matrices. I make use of this special case in combination of the proxy VAR with the Max-Share framework where I point identify two shocks with restrictions on only one of the two shocks.

To avoid confusion, in the following sections every rotation matrix is of dimension $l \times l$. For the parts describing identification of the proxy VAR with the Max-Share approach $l = 2$.

3 Proxy VAR with Restrictions on the FEV

3.1 Proxy VARs with Bounds on the FEV

The bounds on the contributions to the FEV where introduced by Volpicella (2021) and this section applies them to the proxy SVAR framework. In doing so, I loosely follow the notation of Volpicella (2021). Such bounds on the FEV are inequality restrictions in the spirit of the well known sign restrictions on impulse response parameter, an thus the structural parameters are set identified. Naturally, the challenges the set identification literature deals with also apply to this identification scheme.

3.1.1 Bounding the contribution to the FEV

In the proxy VAR framework the contribution of shock j to the FEV of variable i at horizon h is:

$$\Omega_{ij}(h) = \frac{e_i'(\sum_{m=0}^{h-1} C_m B_z q_j q_j' B_z' C_m')e_i}{e_i'(\sum_{m=0}^{h-1} C_m \Sigma C_m')e_i}. \tag{22}$$

Uhlig (2004b) shows that equation (22) can also be written as:

$$\Omega_{i,j}(h) = q_j' R_{i,h} q_j, \tag{23}$$

where

$$R_{i,h} = \frac{\sum_{m=0}^{h-1} c_{i,m}' c_{i,m}}{e_i'(\sum_{m=0}^{h-1} C_m \Sigma C_m')e_i}, \tag{24}$$

with $c_{i,m} = e_i C_m B_z$ is the ith row vector of $C_m B_z$. $R_{i,h}$ is a positive semidefinite and symmetric $l \times l$ real matrix.

Given equation (23) the bounds on the contribution to the FEV of variable i by shock j at horizon h can be represented by:

$$\underline{\tau}_{i,j,h} \leq q_j' R_{i,h} q_j \leq \overline{\tau}_{i,j,h},$$

where $\underline{\tau}_{i,j,h}$ and $\overline{\tau}_{i,j,h}$ depict the lower and upper bound, respectively, and $0 \leq \underline{\tau}_{i,j,h} \leq \overline{\tau}_{i,j,h} \leq 1$. Let $\mathcal{I}_j$ be a set of indices that depict whether the FEV of variable i is bounded and $\mathcal{H}_{ij}$ collects the horizons $h = 0, 1, ...$ for which these bounds are imposed. The whole set of bound constraints is then characterized by

$$\underline{\tau}_{i,j,h} \leq q_j' R_{i,h} q_j \leq \overline{\tau}_{i,j,h}, \text{ for } i \in \mathcal{I}_j \text{ and } h \in \mathcal{H}_{ij}.$$

These bounds on the contributions to the FEV can also be applied together with already existing set identifying inequality restrictions, like e.g. sign restrictions. Furthermore, restrictions on the correlations of the proxies with the identified shocks are possible. These type of restrictions constrain the elements of Ψ. They can be checked employing the routine used by Piffer and Podstawski (2018). The identified set is then characterized by all the rotation matrices Q for which these FEV bounds and other potential restrictions are satisfied. As pointed out by Volpicella (2021) such bounds on the FEV contributions can be derived either through economic theory or simply by strong beliefs due to economic intuition.

3.1.2 Nonemptiness of the Set

The bound restrictions, together with potential additional restrictions, are subject to set-identification specific considerations. On the one hand, if the bounds are not restrictive enough one gets potentially large identified sets which yield a fuzzy identification of the underlying structural effects. If, on the other hand, the bounds are to restrictive the identified set might be empty because no structural representation of the model satisfies them.

Unfortunately, no formal guidance helps to assess the restrictions in this regard, what in turn highlights the importance of the economic theory or intuition behind them. Yet, if the identified set is empty, this might be a sign that the imposed restrictions are not reasonable.

Furthermore, it is important to know whether the set is empty for the estimation procedure. Volpicella (2021) provides sufficient conditions for the nonemptiness of the identified set when only one shock is restricted. These sufficient conditions also apply in the same fashion to the proxy VAR framework. Recall that the contribution of the target shock j to the FEV of variable i is:

$$\Omega_{ij}(h) = q_j' R_{i,h} q_j, \tag{25}$$

Let λ_m^{ih} the real eigenvalues of $R_{i,j}$ with $i \in \mathcal{I}_j$, $h \in \mathcal{H}_{ij}$ and $m = 1, ..., l$. Uhlig (2004b) shows that finding the maximum (minimum) of (25) with respect to q_j amounts to finding the largest (smallest) eigenvalue λ_m^{ih} of $R_{i,j}$ and the maximum (minimum) is achieved by using the corresponding eigenvector q_m as a rotation vector q_j. Hence, the eigenvalues λ_m^{ih} correspond to the contributions to the FEV of variable i at horizon h.

Proposition 3.1 follows from Proposition 3.1 of Volpicella (2021) and gives sufficient conditions for the nonemptiness of the identified set when a single target shock j is restricted.

Proposition 3.1. (Nonemptiness) If the following conditions hold:

(a) $\exists i \in \mathcal{I}_j, \exists h \in \mathcal{H}_{ij} \mid \underline{\tau}_{i,j,h} \leq \lambda_m^{ih} \leq \overline{\tau}_{i,j,h},\ Rq_m = \lambda_m^{ih} q_m$ for some $m = 1, ..., l$,

(b) given q_m from (a), $\underline{\tau}_{i,j,h} \leq q_m' R_{i,h} q_m \leq \overline{\tau}_{i,j,h} \forall i \in \mathcal{I}_j$ and $\forall h \in \mathcal{H}_{ij}$, and all other additional restrictions are satisfied,

then the identified set is non-empty and bounded.

If the contribution to the FEV of a single variable i is bounded the condition reduces to a simple check whether one of the eigenvalues λ_m^{ih} lies within the bounds. When additional restrictions, like sign restrictions, are imposed one also has to check whether they are satisfied for $q_j = q_m$.

Apart from Volpicella (2021) Proposition 3.1 not only applies when only one shock is constrained. In the special case of $l = 2$, Proposition 3.1 also helps to detect nonemptiness also when both shocks are subject to identification restrictions. Knowing q_m amounts to knowing the whole 2×2 rotation matrix Q_m due to the properties of orthonormal matrices. Hence, in step (b) of Proposition 3.1 also the restrictions on the second shock can be checked.

Another difference to Volpicella (2021) is the number of eigenvalues that are available for assessment of the nonemptiness. In the proxy VAR only l eigenvalues are at hand compared to the k eigenvalues in Volpicella (2021). In practice the sufficient conditions will be met more frequently compared to the case with only l eigenvalues. On top of that, the largest and smallest eigenvalue in the proxy VAR case represents the maximum and minimum contribution to the FEV at the specific horizon. Hence, if $l = 2$ only the maximum and minimum contribution can be used to check the nonemptiness. If the bounds do not encompass the extreme values the sufficient conditions are not satisfied. Yet, in practice it might be interesting to set the bounds on the FEVD such that they are close to the maximum or minimum and the empirical illustration highlights this case.

If the sufficient conditions of Proposition 3.1 are not fulfilled a different approach helps to approximate the nonemptiness of the identified set. As often done in the literature, one can draw a specified number of matrices Q from the orthonormal space. If none of this draws satisfies the restrictions one can conclude that the set is empty.

Lastly, one can see that the set is empty if the upper bound $\overline{\tau}_{i,j,h}$ is smaller than the minimum eigenvalue for one of the imposed bounds, or if the lower bound $\underline{\tau}_{i,j,h}$ is larger than the maximum eigenvalue. In these cases the just mentioned alternative is obsolete.

3.1.3 Estimation and Inference

This subsection introduces the robust bayesian inference framework by Giacomini et al. (2021). The benefit of this approach is that it avoids specifying a prior over the rotation matrices Q that is not updated by the data. Baumeister and Hamilton (2015) show that when the prior for the rotation matrices Q is a uniform distribution over that space of orthonormal matrices, the common approach in the literature, the structural parameters are influenced by the prior distribution even asymptotically.

The remedy is to use a distribution-free approach. In the robust bayesian inference the endpoints of the identified set are calculated numerically or analytically if possible. The endpoints, or boundaries, of the identified set are the maximum and minimum values of the structural parameters of interest given all admissible rotation matrices Q. Giacomini et al. (2021) show that this procedure yields prior

robust inference over the structural parameters.

As mentioned previously, I adapt the algorithm used in Giacomini et al. (2021) to the specification of the proxy VAR framework in the previous section. I incorporate the exogeneity and relevance restriction regarding the proxies via the proxy impact matrix B_z and only rotate the upper block B_{11} with an orthonormal matrix Q. Apart from the benefit that I can fit bounding the FEVD and the Max-Share approach in the same proxy VAR framework, two additional advantages arise. One merit is that I do not need to draw the rotation matrices Q subject to the exogeneity restriction as depicted in (13). For large iteration counts of the inference algorithm this potentially saves some computation time. Further, I avoid a specific ordering of the variables in the VAR. The ordering convention defined in Giacomini et al. (2021) might be difficult to incorporate in practice when it is not obvious which structural shock is linked to which variable in the VAR system.

To describe the bayesian algorithm let $\phi \in \Phi$ collect all the reduced form parameters in (2) and (12). For the following algorithm it is not important which prior for ϕ is used as long as one is capable to draw from the posterior distribution of the reduced form parameters. For the results derived in the next sections I follow Giacomini et al. (2021) and use an (improper) Jeffrey's prior.

Suppose that the impulse responses $\eta_{i,j,h} = e_i' C_m B_z q_j$ are the structural parameters of interest. The upper and lower boundary of the identified set with respect to the imposed restrictions are depicted by $u_{i,h}(\phi)$ and $l_{i,h}(\phi)$. Algorithm 1 describes how to conduct robust bayesian inference for the identified set of $\eta_{i,j,h}$.

Algorithm 1.

Step 1: Obtain draws ϕ from its posterior distribution and compute B_{11}^c.

Step 2: Check whether the identified set is empty. If the set is empty go back to Step 1. If the set is non-empty proceed with Step 3.

Step 3: Compute the boundaries of the identified set:

$$
\begin{aligned}
l_{i,h}(\phi) = \min_{Q} \; & e_i' C_m B_z q_j \\
s.t \quad & \underline{\tau}_{i,j,h} \leq q_j' R_{i,h}(\phi) q_j \leq \overline{\tau}_{i,j,h}, \quad \forall i \in \mathcal{I}_j \text{ and } \forall h \in \mathcal{H}_{ij}, \\
& QQ' = I_l, \\
& \text{potential sign restrictions and/or restrictions on } \Psi.
\end{aligned}
$$

The upper boundary $u_{i,h}(\phi)$ is obtained analogously.

Step 4: Repeat Steps 2 and 3 N times.

Step 5: Approximate the set of posterior means and the robust credible region as described in Giacomini et al. (2021).

Especially, Step 2 differs from the algorithm of Giacomini et al. (2021) as Proposition 3.1 helps to gauge whether the identified set is empty. If the sufficient conditions of Proposition 3.1 are not fulfilled a specified number of rotation matrices Q are drawn to approximate the set as being empty if none of the draws satisfies the identification restrictions. In this case, Step 2 differs from Giacomini et al. (2021) as the $l \times l$ rotation matrices Q do not need to be drawn considering the exogeneity conditions for the proxies. These conditions are already incorporated in the construction of B_z. Step 3 differs in the specification of the proxy VAR, and thus the dimension of the rotation matrix Q. Second, the added constraint in the maximization problem that represents the restrictions on the FEV are a distinction to the algorithm in Giacomini et al. (2021).

Step 3 poses a nonconvex optimization problem. Hence, the typical approaches to handle with gradient based optimization techniques are necessary. The simple remedy is to use different initial values and to compute the maximum or minimum over the set of solutions which are derived with the different initial values.

Giacomini et al. (2021) also provide an algorithm to approximate the boundaries of the identified set in order to check the convergence of the numerical optimization or simply as an alternative.

Algorithm 2. Replace Step 3 of Algortihm 1 with:

Step 3: Draw Q until N draws hat satisfy the identification restrictions are reached. For each $Q_n,\ 1, ..., N$ compute $\eta_{n,i,j,h} = e_i' C_m B_z q_{n,j}$ and approximate $u_{i,h}(\phi)$ and $l_{i,h}(\phi)$ by the maximum and minimum of $\eta_{n,i,j,h}$ over all N draws.

Montiel Olea and Nesbit (2021) show that the random sampling approximation of Algorithm 2 can be represented as a supervised learning problem. They provide the number of admissible draws of Q that are needed to learn the set with a certain precision. Generally, the approximated set will be smaller than the true set, yet with a sufficient amount of draws the approximation error will be small. The theoretical results of Montiel Olea and Nesbit (2021) can be used to judge the precision of the approximation at a certain amount of draws N.

Giacomini et al. (2021) argue that this approximation might be favourable under certain circumstances. Firstly, if the VAR system is large and one is interested in the impulse responses for many variables at many horizons. Drawing many rotation matrices Q is computationally less costly than optimizing for every variable at every horizon. This is especially true with the representation of the proxy VAR used in this paper as it is quite easy to draw simple $l \times l$ rotation matrices considering that l is small in most empirical applications. Second, if not only the impulse

responses but also e.g. the FEV decomposition is of interest the approximation has an advantage. Each draw of Q can be used to compute the impulse responses and FEV decomposition of each variable at every horizon, while the optimization has to be carried out for each parameter, variable and horizon individually.

3.2 Proxy VAR and Max-Share

This sections describes how the shocks in the proxy VAR can be disentangled using the Max-Share framework that was introduced by Faust (1998) and Uhlig (2004b). The key assumption behind the Max-Share approach is, that the shock of interest j is the one that maximizes the contribution to the FEV of a target variable i. This amounts to finding the rotation vector q_j for which this maximum is achieved:

$$q_j^* = \text{argmax} \sum_{h=0}^{H} \Omega_{i,j}^z(h) \quad \text{s.t.} \quad q_j' q_j = 1. \tag{26}$$

In the proxy VAR, $\Omega_{i,j}^z(h)$ is given by:

$$\Omega_{i,j}^z(h) = \frac{e_i'(\sum_{m=0}^{h-1} C_m B_z q_j q_j' B_z' C_m')e_i}{e_i'(\sum_{m=0}^{h-1} C_m \Sigma C_m')e_i}, \tag{27}$$

where q_j is the jt column of the $l \times l$ orthonormal matrix Q. The closed form solution of the maximization problem shown by Uhlig (2004b) also applies to the proxy VAR case in (26).

Yet, recently Dieppe et al. (2019) highlighted that this identification assumption fails if another shock also contributes to the FEV of the same target variable. To give an example assume that the technology shock is accountable for most of the FEV of a total factor productivity (TFP) measurement. If then the technology shock is identified as the shock that maximizes the contribution to the TFP measurement, the results will be biased because also other shocks contribute to the same FEV. Dieppe et al. (2019) present strategies how to circumvent this problem of confounding shocks in the baseline Max-Share identification without proxies. In this section I focus on the remedies to the bias concerns that the proxy VAR framework offers.

3.2.1 Ruling out Confounders via the Proxy VAR

First and foremost, the proxy VAR helps with the confounding shocks as it rules out confounding shocks that are not related to the proxies. For example, assume two proxies are used to identify two shocks. One of the shocks contributes the most to the FEV of a specified variable and out of the two shocks that are related to the proxies it contributes exclusively to the FEV of this variable. Suppose another

shock that is not related to the proxies also contributes to the FEV of this target variable. Yet, as it is not related to the proxies it is ruled out as a confounding shock. As out of the two shocks that are related to the proxies only one exclusively contributes to the FEV of the target variable, the Max-Share framework correctly disentangles the shocks of interest.

This particular example is depicted in the simulation study of the next section and provides evidence that the proxy VAR rules out potentially confounding shocks. (More to come)

3.2.2 Reducing the Bias - Two Shocks

In the special case of two shocks additional inequality restrictions can tackle bias concerns even when both shocks related to the proxies contribute to the FEV of the target variable. In practice the case of to instruments is highly relevant, as finding multiple convincing proxy variables is difficult and finding two of them is already a challenging task. If two shocks are identified using two instruments the rotations matrix Q has dimension 2×2. Then identifying the first column of a 2×2 orthogonal matrix also identifies the second column up to a sign normalization due to the properties of orthonormal matrices:

$$Q = \begin{pmatrix} q_{11} & q_{12} \\ q_{21} & q_{22} \end{pmatrix}, \qquad 1 = q_{21}^2 + q_{22}^2 \quad \text{and} \quad 1 = q_{11}^2 + q_{12}^2. \tag{28}$$

Hence, the identification of one shock via the Max-Share framework also gives the structural parameters of the second shock. Suppose, the first shock is identified with the Max-Share strategy, then the impulse responses of the second shock are pinned down up to sign. Recall, that the structural impulse response of variable i to the first shock at horizon h is given by:

$$\eta_{i,1,h} = e_i' C_h B_z q_1.$$

The additional inequality restriction that I propose restricts the relative magnitude of the impulse response of the same variable to the two shocks in the system. The corresponding augmented optimization problem for the Max-Share strategy is given by:

$$q_j^* = \text{argmax} \sum_{h=0}^{H} \Omega_{i,j}^z(h) \tag{29}$$

$$\text{s.t.}$$

$$q_1' q_1 = 1,$$

$$q_1' q_2 = 0,$$

$$\eta_{i,1,0} - \eta_{i,2,0} > \epsilon,$$

where $\eta_{i,1,0}$ and $\eta_{i,2,0}$ are the contemporaneous responses of variable i to the first and second shock, respectively.

Two things regarding this added inequality restriction have to be accounted for. Firstly, the added restriction has to be binding. To see if the restriction is binding one first has to compute the biased results using the basic Max-Share strategy (26) in the proxy VAR. Given the biased results one is able to check whether the inequality restriction that wants to be imposed is already satisfied or not. If the restriction is already satisfied including it as in the optimization problem in (29) will not change the biased results as the constraint is not binding. Hence, in practice the first step is to check the biased results in order to see whether a suitable economic intuition can serve as a binding constraint to eliminate the bias. Certainly, it can be the case that given the application no suitable economic intuition is available, and thus the identification via the augmented Max-Share framework fails. Yet, the weaker bound restrictions on the FEV, described in the previous section, can serve as an alternative to the more strict Max-Share setting in these cases.

Second, specifying the margin ϵ by which the response to one shock exceeds the one to the other shock is difficult in practice. Even with a sound economic intuition on the relative magnitudes of the responses it is probably hard to have an intuition for the margin ϵ. Thus, I propose to specify a range for ϵ for which one is confident that the true margin is contained and report the results for a grid of these ϵ values. The simulation study will depict examples how to assess whether the constraint is binding and also results for different values of ϵ.

Furthermore, it is potentially possible to restrict other horizons of the impulse responses as well. This needs to be explored further. However, it is most likely easier to argue with the initial responses in practice.

3.2.3 Estimation and Inference

The combination of the proxy VAR with the Max-Share framework can also be handled with the bayesian Algorithm 1 that was depicted above. In combination with

the Max-Share framework, steps two and three are simply replaced with carrying out the Max-Share optimization. Note that this reduces the robust bayesian approach to conventional bayesian inference. Step three in Algorithm 1, the core of the robust bayesian inference, computes the boundaries of the identified set and in the point identification case the identified set is a singleton. Hence, computing the bounds reduces to the computation of the point estimate.

However, in point identification scheme bootstrap inference is popular. In this case, I propose the bootstrap by Jentsch and Lunsford (2019a), which is based on the heteroskedasticity robust bootstrap by Brüggemann, Jentsch, and Trenkler (2016). This approach relies on estimating Z and Σ to get an estimate for B_{11}^c (see Piffer & Podstawski, 2018). The bootstrap confidence intervals are constructed in the conventional way.

4 Simulation Results

In the simulation studies of this section I simulate a trivariate system. I follow Piffer and Podstawski (2018) and use the New Keynesian model by An and Schorfheide (2007) and Komunjer and Ng (2011). The model contains interest rates r_t, output x_t and inflation π_t. TFP shocks w_t^z, government spending shocks w_t^g and monetary shocks w_t^r are the structural shocks that hit the system. As pointed out by Giacomini (2013), calibrating the parameter gives following DGP:

$$\begin{pmatrix} r_t \\ x_t \\ \pi_t \end{pmatrix} = \begin{pmatrix} 0.79 & 0 & 0.25 \\ 0.19 & 0.95 & -0.46 \\ 0.12 & 0 & 0.62 \end{pmatrix} \begin{pmatrix} r_{t-1} \\ x_{t-1} \\ \pi_{t-1} \end{pmatrix} + \begin{pmatrix} 0.61 & 0 & 0.69 \\ 1.49 & 1 & -1.16 \\ 1.49 & 0 & -0.75 \end{pmatrix} \begin{pmatrix} w_t^z \\ w_t^g \\ w_t^r \end{pmatrix}. \tag{30}$$

In contrast to Piffer and Podstawski (2018) I set the variance of the structural shocks to unity in order easily compute the actual contribution to the FEV decomposition. Hence, the structural shocks are drawn from a normal distribution with mean zero and unit variance and then used to simulate the data with equation (30). The instruments are constructed with:

$$\begin{aligned} m_{1t} &= \tau_1 w_t^z + (1-\tau_1) w_t^g + \tau_2 \nu_{1t} \\ m_{2t} &= (1-\tau_1) w_t^z + \tau_1 w_t^g + \tau_2 \nu_{2t}, \end{aligned}$$

where τ_1 governs the strength of the relation of the first to shocks with the instruments and τ_2 governs the effect of the white noise disturbances ν_{1t} and ν_{2t}. I set $\tau_1 = 0.55$ and $\tau_2 = 0.01$ which leads to the proxies being sufficiently strong.

The technology shock w_t^z is accountable for the most part of the FEV of the interest rate r_t. An interesting feature of this DGP is that the government spending shock does not contribute to the FEV of the interest rate and inflation at any horizon. This enables me to construct two scenarios:

> *Scenario A:* The proxies are constructed such that they are related to the technology shock $_t^z$ and the government spending shock w_t^g. Out of this two shocks w_t^z contributes exclusively to the FEV of the interest rate r_t.
>
> *Scenario B:* The proxies are constructed such that they are related to the technology shock w_t^z and the monetary policy shock w_t^r. Both of this two shocks contribute to the FEV of the interest rate r_t.

These two scenarios will be if particular interest for the subsection in which the shocks are disentangled with the Max-Share approach.

4.1 Simulation Results - Bound Restrictions

To come.

4.2 Simulation Results - Max-Share

This subsection presents the simulation results for the case when to shocks are disentangled in the proxy VAR. The first results compare Scenario A and B which were described above. In Scenario A out of the two identified shocks, only the technology shocks contributes to the FEV of the interest rate. In Scenario B both shocks contribute to the FEV of the interest rate. Up to horizon $H = 13$ the technology shock w_t^z contributes on average 82%, the government spending shock w_t^g does not contribute to the FEV and the monetary policy shock w_t^r contributes the remaining 18%. In this section the interest rate is always the target variable in the Max-Share framework. Hence, the underlying assumption is that the technology shock is the one that maximizes the contribution to the FEV of the interest rate.

Table 1 depicts the results for the identification via maximization of the FEV after incorporating the information of the instruments as in (26) and without further inequality restrictions on relative magnitudes. As this is more of a confirmation exercise in which cases the Max-Share approach succeeds and fails I choose a large sample size of $T = 1,000$ with $M = 1,000$ Monte-Carlo iterations. The first two columns of the table show the true structural parameters of the DGP, the next two columns the combination of proxy VAR and Max-Share and the last two the identification via the Cholesky decomposition as in e.g. Mertens and Ravn (2013), i.e. $B_{11} = B_{11}^c$ is lower triangular. Looking at the results for Scenario A shows that

after incorporating the proxies the shock that is not related to them is purged from the maximization problem. Only the two shocks that are related to the instruments are factored in and as one of the shocks contributes exclusively to the FEV of the target variable the Max-Share approach is suitable to disentangle these two. Yet, this set-up with exclusive contribution implies a recursive structure for the contemporaneous impacts of the shock, and thus the Cholesky decomposition for the upper 2×2 block of the proxy impact matrix will also identify the true underlying structural parameters.

Hence, the potentially more interesting case is when both identified shocks contribute to the FEV of the target variable as in Scenario B. As seen in the panel for Scenario B of Table 1, the Cholesky decomposition fails to identify the true impact matrix as there is no recursive structure between the two identified shocks. However, as expected also the combination of the proxy VAR with the Max-Share approach yields biased results because both shocks contribute to the FEV of the target variable. As pointed out by Dieppe et al. (2019), the Max-Share framework will be biased due to the confounding shock.

To successfully disentangle the two shocks when both shocks contribute to the FEV, the Max-Share framework needs to be augmented. As mentioned above, I propose to use restrictions on the contemporaneous responses of a specified variable. For the illustrative purpose I restrict the relative contemporaneous response of out-

Table 1: Two Shocks without Exclusive Contribution

DGP		Proxy + Max-Share		Proxy + Cholesky	
Scenario A					
0.61	0	0.609	0.004	0.609	0
		(0.007)	(0.004)	(0.007)	(0)
1.49	1	1.487	1.014	1.485	1.004
		(0.016)	(0.036	(0.012)	(0.03)
1.49	0	1.488	0.015	1.488	0.004
		(0.008)	(0.008)	(0.008)	(0.023)
Scenario B					
0.61	0.69	0.766	0.512	0.921	0
		(0.008)	(0.004)	(0.006)	(0)
1.49	-1.1	1.161	1.624	0.163	1.845
		(0.021)	(0.019	(0.022)	(0.016)
1.49	-0.75	1.25	1.578	0.426	1.6131
		(0.016)	(0.014)	(0.017)	(0.011)

The table depicts the average of the estimated structural parameters over the 1,000 Monte-Carlo simulation iterations derived with the proxy SVAR. The shocks are once disentangled with the baseline Max-Share approach and once with the Cholesky decomposition. The value in the bracket depicts the respective standard deviation.

put to the two identified shocks. In this DGP, a common, one standard deviation, expansionary technology shock has a more pronounced positive effect (1.49) than a common expansionary monetary policy shock (1.1). Augmenting the maximization problem such that this inequality constraint holds helps to disentangle the two shocks.

Yet, as pointed out before the constraint needs to be binding, meaning that the biased results of the basic combination of proxy VAR and Max-Share in (26) do not already satisfy this relation between the shocks. Looking at Scenario B in Table 1, one sees that the contemporaneous response of output to the technology shock is $\eta_{2,1,0} = 1.161$ while the response to the monetary shock is $\eta_{2,2,0} = 1.6124$. The constraint that the contemporaneous response to the technology shock has to be

Table 2: Max-Share with Additional Inequality Constraint - Scenario B

DGP		Max-Share$^+$, T=1000		Max-Share$^+$, T=250	
Panel A: $\epsilon = 0.38$					
0.61	0.69	0.613	0.688	0.612	0.688
		(0.029)	(0.026)	(0.057)	(0.052)
1.49	-1.1	1.486	-1.106	1.481	-1.101
		(0.044)	(0.044)	(0.087)	(0.087)
1.49	-0.75	1.487	-0.755	1.483	-0.755
		(0.031)	(0.038)	(0.062)	(0.075)
Panel B: $\epsilon = 0.2$					
0.61	0.69	0.659	0.644	0.658	0.643
		(0.027)	(0.027)	(0.055)	(0.054)
1.49	-1.1	1.406	-1.206	1.405	-1.205
		(0.044)	(0.045)	(0.075)	(0.074)
1.49	-0.75	1.432	-0.856	1.429	-0.858
		(0.032)	(0.037)	(0.062)	(0.072)
Panel C: $\epsilon = 0$					
0.61	0.69	0.706	0.592	0.706	0.591
		(0.026)	(0.027)	(0.053)	(0.055)
1.49	-1.1	1.311	-1.311	1.31	-1.309
		(0.037)	(0.037)	(0.075)	(0.074)
1.49	-0.75	1.362	-0.963	1.36	-0.965
		(0.032)	(0.036)	(0.063)	(0.07)

The table depicts the average of the estimated structural parameters over the 1,000 Monte-Carlo simulation iterations. The estimates are derived with the Max-Share$^+$ framework in the proxy VAR with different values of ϵ.

larger is binding in this case. Note that for this example the bias is such that every variable could be used.

In order to impose such a constraint, one would need to argue that from prior knowledge or economic theory it is known that the common expansionary technology shock affects output more than the common expansionary monetary policy shock on impact. Without knowledge about the true DGP this margin ϵ is typically unknown and needs to be gauged by the researcher.

The full maximization problem for this particular simulation with the just mentioned restrictions is:

$$
\begin{aligned}
& q_1^* = \text{argmax} \sum_{h=0}^{H} \Omega_{1,1}^z(h) && (31)\\
& \text{s.t.} \\
& q_1' q_1 = 1, \\
& q_1' q_2 = 0, \\
& \eta_{2,1,0} - (-\eta_{2,2,0}) > \epsilon, \\
& \eta_{2,1,0} > 0, \\
& \eta_{2,2,0} > 0.
\end{aligned}
$$

Table 2 depicts the results for this augmented Max-Share identification, denoted by Max-Share$^+$. The first two columns again depict the true DGP parameters, while columns three and four give the results of the Max-Share$^+$ framework with $T = 1000$ while the last two columns give the results for $T = 250$. Panel A shows the results for $\epsilon = 0.38$ which is very close to the true margin by which $\eta_{2,1,0}$ exceeds $\eta_{2,2,0}$ in absolute terms. Panel B shows the results for $\epsilon = 0.2$ and Panel C the results for $\epsilon = 0$. The latter represents the case when restriction boils down to a sign restriction on the relative magnitudes of the two shocks.

Comparing the estimates throughout the panels reveals that having the (almost) correct economic intuition with the inequality restriction ($\epsilon = 0.38$) removes almost all of the bias of the Max-Share approach. Yet, if the true margin is not met part of the bias remains and it is larger the less close the true margin is met. This is true for both the technology as well as the monetary policy shock.

Comparing the results in terms of the sample sizes shows that even for smaller sample sizes like $T = 250$ the true structural parameters are identified reliably with the correct economic intuition. Naturally, the bias also remains for smaller sample sizes when ϵ is not very close to the true margin.

Figure 1 and 2 show the 2,5% and 97,5% quantiles (dashed lines) of the estimated impulse responses identified by the augmented Max-Share throughout the 1,000

Figure 1: 95% Point Estimate Bands, $\epsilon = 0.38$ - Scenario B

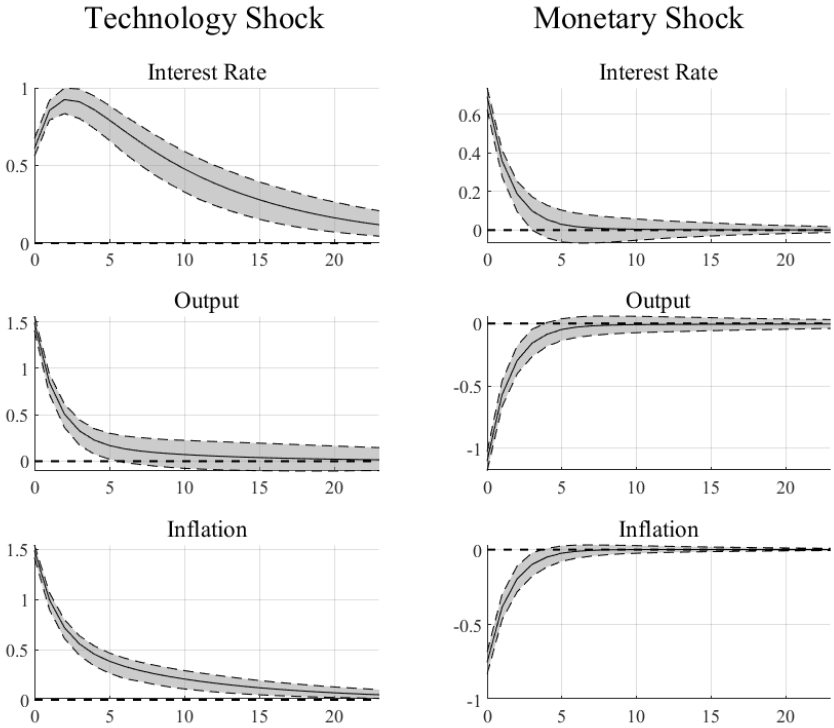

The solid lines depict the true impulse responses of the DGP. The dashed lines are the 2,5% and 97,5% quantile of the solutions found for the 1,000 Monte-Carlo simulation iterations.

Monte-Carlo simulation rounds. The true impulse responses are depicted by the solid lines. Figure 1 presents the responses obtained with the $\epsilon = 0.38$, close to the true margin while Figure 2 presents the results for $\epsilon = 0$. The impulse responses for $\epsilon = 0.2$ can be found in the Appendix B.

The figures are in line with the results of Table 2. The estimated responses in Figure 1 closely identify the true structural impulse response parameters while the responses in Figure 2 reflect the bias of the impact matrix parameters in the bias of the impulse responses especially at earlier horizons. As the horizon of the responses increases the bias sees to shrink.

The bias of the structural impulse responses at different horizon and for different values of ϵ is depicted in Table 3 for the technology shock and in Table 4 for the monetary policy shock. Comparing the results throughout the panels the bias is larger when ϵ is farther away from the true margin. Comparing the results along the columns shows that the bias is typically larger for earlier horizons of the responses and is small at later horizons. These patterns are consistent throughout both tables, and therefore both identified shocks. Results for $T = 250$ are presented to the Appendix B.

Figure 2: 95% Point Estimate Bands, $\epsilon = 0$ - Scenario B

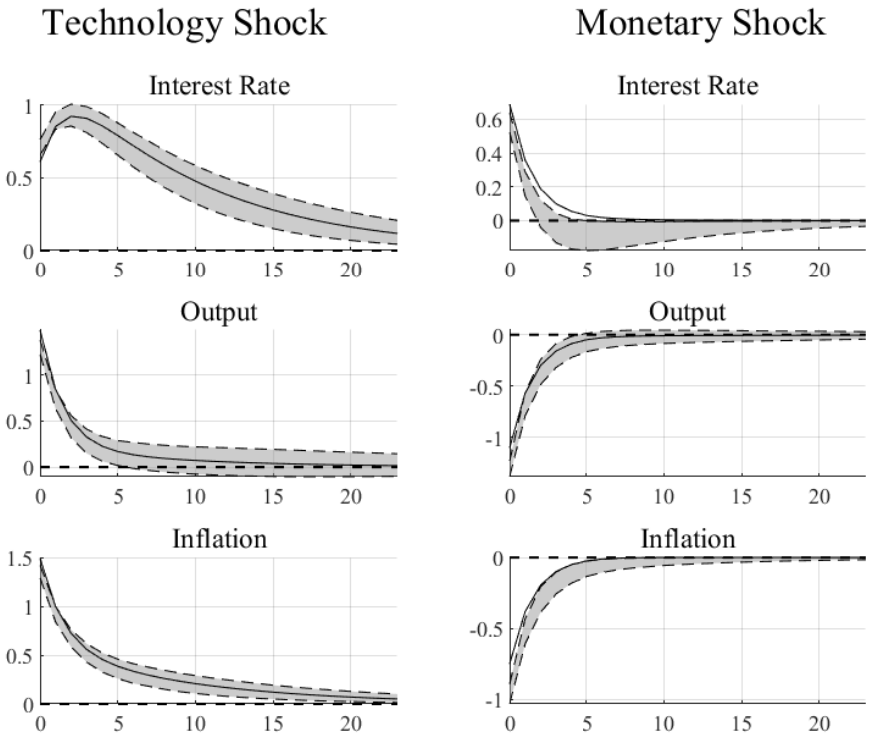

The solid lines are the true impulse responses of the DGP. The dashed lines are the 2,5% and 97,5% quantile of the solutions found for the 1,000 Monte-Carlo simulation iterations.

The patters found in Tables 3 and 4 are visualized in Figures 3 and 4. The coloured lines depict the bias of the structural impulse responses at different horizons and for different values of ϵ. The same visualization for $T = 250$ is again relegated to the Appendix B.

Lastly, the additional constraints in the maximization problem (29) or (31) can also serve a pure inequality restrictions in order to set identify the shocks. Hence, one could also try to disentangle the shocks in the Proxy VAR with this inequality restrictions. The resulting sets of impulse responses are depicted in Figure 13 of the Appendix. The picture shows that the use of the Max-Share framework helps to estimate the structural impulse responses more precisely, as the simulated sets are rather wide compared to the range of simulated point estimates of the Max-Share approach for the majority of the impulse responses.

Table 3: Bias of the IRFs to the Technology Shock, $T = 1000$ - Scenario B

Variable	$H = 0$	$H = 6$	$H = 12$	$H = 18$
Panel A: $\epsilon = 0.38$				
r_t	0.0025	-0.0178	-0.0198	-0.0136
x_t	-0.0045	-0.0108	-0.0055	-0.0018
π_t	-0.0026	-0.0146	-0.0113	-0.0065
Panel B: $\epsilon = 0.2$				
r_t	0.0486	-0.0186	-0.0207	-0.014
x_t	-0.0844	-0.0131	-0.0061	-0.0022
π_t	-0.0584	-0.0163	-0.0117	-0.0067
Panel C: $\epsilon = 0$				
r_t	0.0958	-0.0233	-0.0235	-0.0154
x_t	-0.1795	-0.016	-0.0068	-0.0025
π_t	-0.1273	-0.0199	-0.0129	-0.0072

The table depicts the average of the estimated structural parameters over the 1,000 Monte-Carlo simulation iterations. The estimates are derived with the Max-Share$^+$ framework in the proxy VAR with different values of ϵ.

Table 4: Bias of the Impulse Response Functions to the Monetary Shock, $T = 1000$.

Variable	$H = 0$	$H = 6$	$H = 12$	$H = 18$
Panel A: $\epsilon = 0.38$				
r_t	-0.0021	-0.0059	-0.0025	-0.0008
x_t	-0.0055	-0.0005	0.0009	0.001
π_t	-0.0051	-0.0029	-0.0007	-0.0001
Panel B: $\epsilon = 0.2$				
r_t	-0.0462	-0.0546	-0.0278	-0.0138
x_t	-0.1056	-0.0088	-0.0025	-0.0007
π_t	-0.1062	-0.0249	-0.0115	-0.0057
Panel C: $\epsilon = 0$				
r_t	-0.0982	-0.1084	-0.0557	-0.0282
x_t	-0.2105	-0.0184	-0.0067	-0.0029
π_t	-0.2135	-0.0491	-0.0234	-0.0119

The table depicts the average of the estimated structural parameters over the 1,000 Monte-Carlo simulation iterations. The estimates are derived with the Max-Share$^+$ framework in the proxy VAR with different values of ϵ.

Figure 3: Bias of the IRFs to the Technology Shock, $T = 1000$ - Scenario B

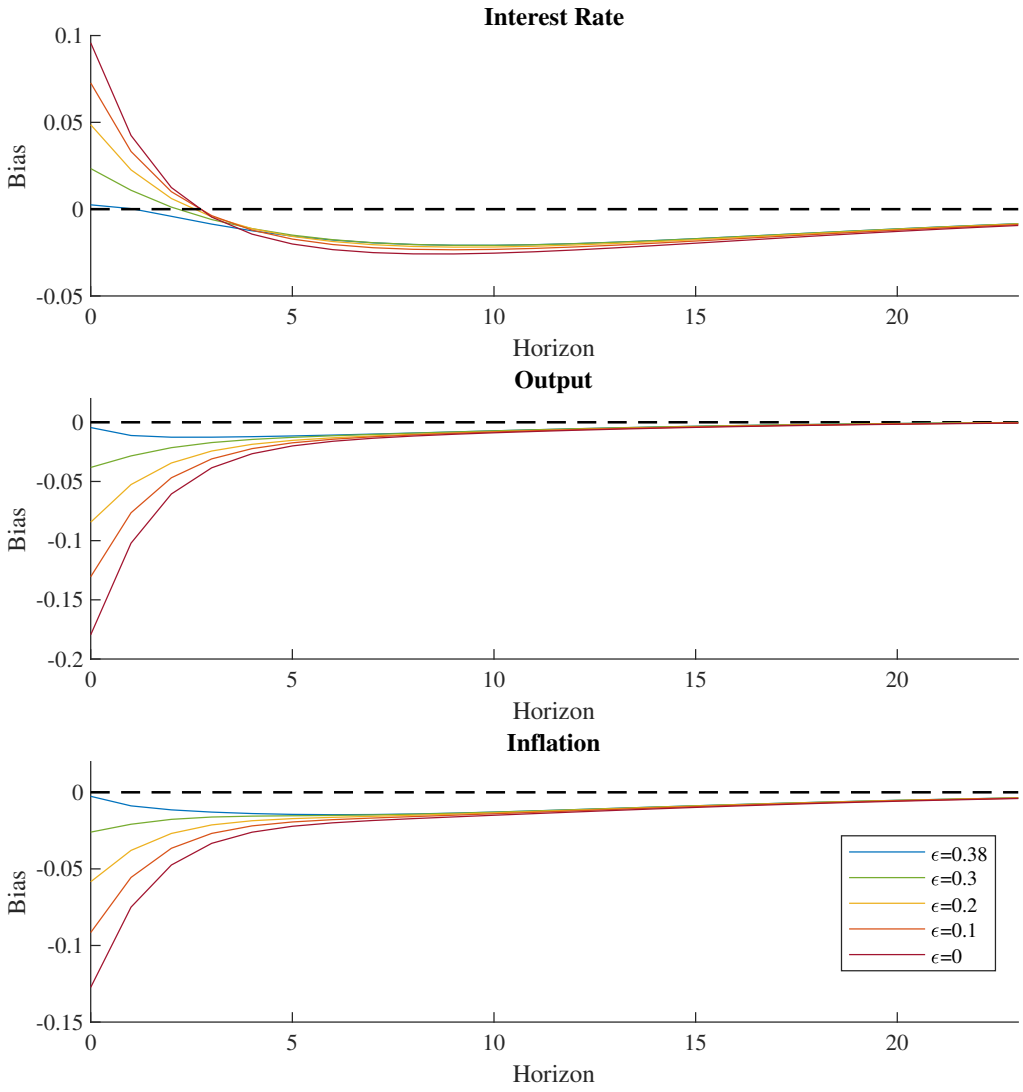

The coloured lines depict the average bias of the impulse response functions over 1,000 Monte-Carlo simulations for different values of ϵ.

Figure 4: Bias of the IRFs to the Monetary Shock, $T = 1000$ - Scenario B

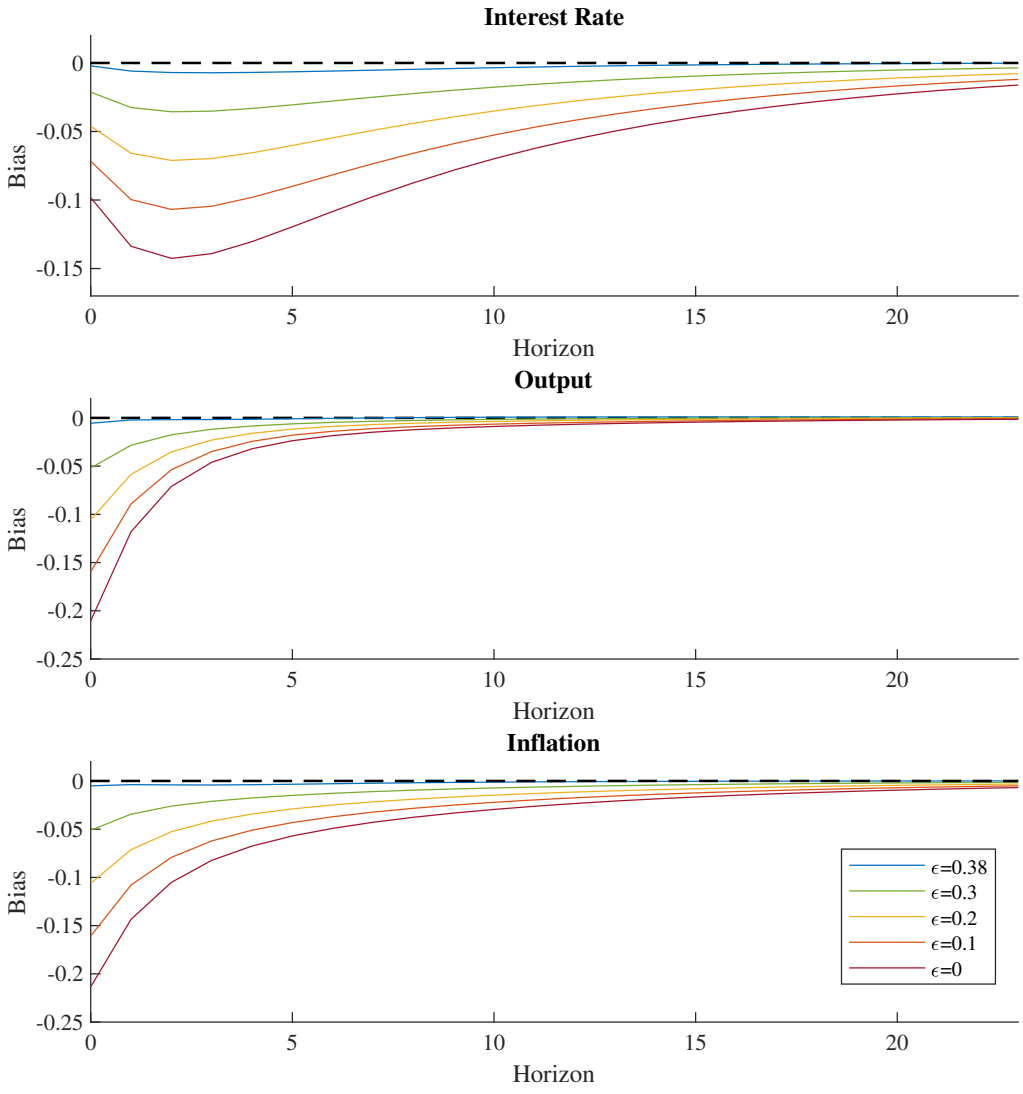

The coloured lines depict the average bias of the impulse response functions over 1,000 Monte-Carlo simulations for different values of ϵ.

5 Empirical Illustration

5.1 Empirical Illustration - Bound Restrictions

An example for an empirical application in which the bounds on the FEV are fitting, is the setting of Mertens and Ravn (2013). They estimate the dynamic causal effects of shocks to the personal and corporate tax rates in the United States. For this purpose their model consists of the personal income tax base, the corporate income tax base, government purchases of final goods, gross domestic product and federal government debt the average personal income tax rate (APITR) ass well as the average corporate income tax rate (ACITR). In this application I adopt the model of Mertens and Ravn (2013), so details about the variables can be found in their study. In order to identify the two tax shocks of interest they construct two proxy variables. They use the list of exogenous tax changes by Romer and Romer (2010) and classify them whether they constitute personal or corporate tax rate changes. Again, I refer the reader to Mertens and Ravn (2013) for further details.

Alongside the relevancy and exogeneity restrictions implied by the proxy VAR, their key identification assumption is that the shock to the personal income tax rate does not affect the ACITR at impact. To check the robustness of the results they also consider the alternative case that APITR does not respond to a shock in the corporal tax rate. This type of equality restriction enables point identification of the two shocks. Yet, the hard equality restrictions need solid reasoning to be convincing. If, for example, legal or political links between personal and corporate taxes exist, the imposed causal ordering of the variables is questionable. Then ACITR would potentially react immediately to a shock in personal taxes and vice versa.

In the literature the results of Mertens and Ravn (2013) sparked some debate. Researches looked, for instance, at weaker identifying restrictions in order to avoid the hard equality restrictions imposed in the original study. E.g. Giacomini et al. (2021) use a mixture of sign restrictions on the correlation matrix ψ and the impulse responses. On top of that they provide robust bayesian inference as an alternative to the frequentist bootstrap confidence intervals employed in Mertens and Ravn (2013) that were also subject to debate in the literature. Jentsch and Lunsford (2019b) provide bootstrap inference that is robust to heteroskedasticity. In summary, these additional iterations of the Mertens and Ravn (2013) study by no means invalidate the results of the original study but rather add layers to the robustness analysis of their results.

This section aims to contribute to this task by transforming equality restrictions imposed by Mertens and Ravn (2013) into a weaker version using bounds on the FEV. Zero equality restrictions on the response of a specific variable at impact are equivalent to imposing that the contribution to the FEV of that variable of the

target shock is zero (see e.g. Volpicella, 2021). Hence, one can weaken the zero restriction in the original study by bounding the contribution of the FEV to be close to zero. In this empirical application I impose that the contribution of the personal (corporate) tax rate shock to the FEV of the ACITR (APITR) is below 5% at impact and for the first three quarters after the shock.

Figure 5: Responses to the APITR shock.

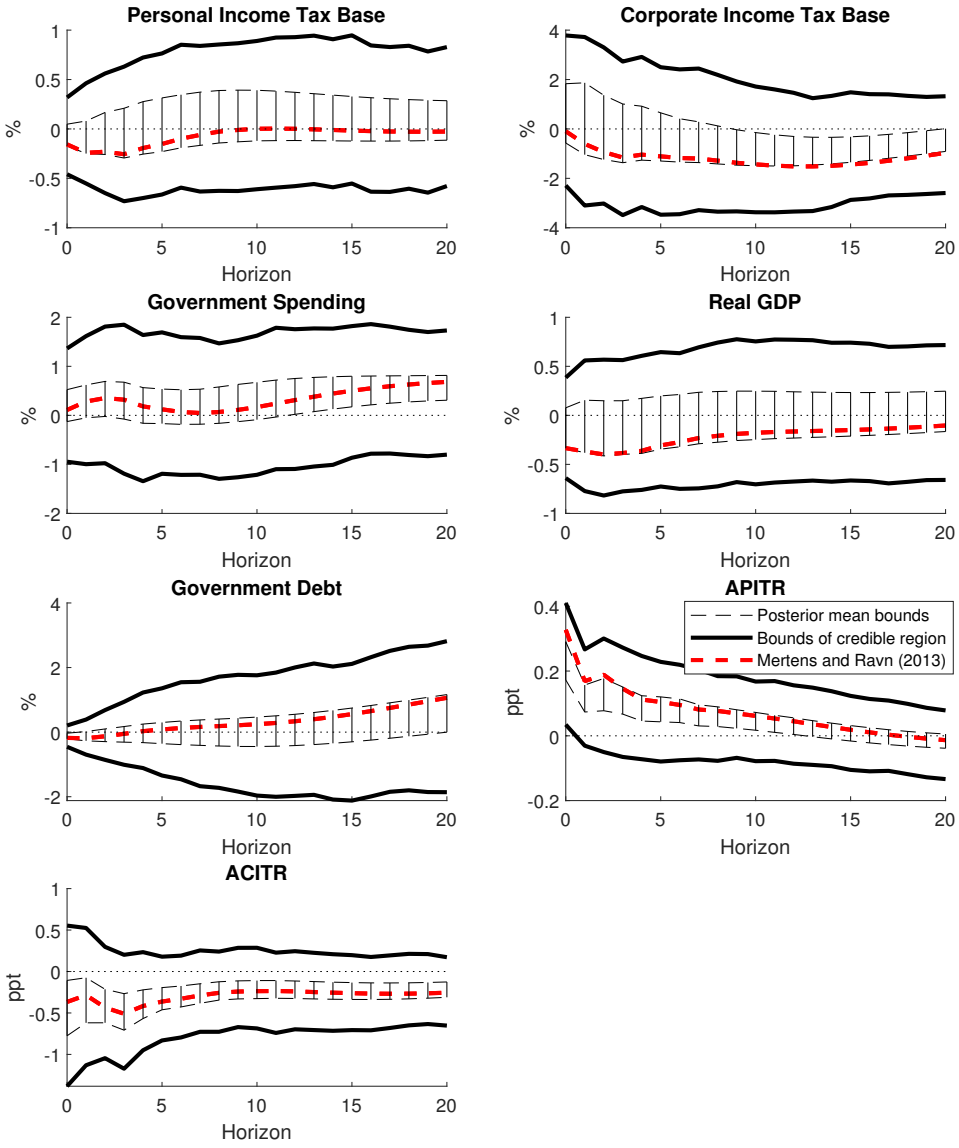

The results are based on 1,000 draws from the posterior of the reduced form coefficients and 1,000 draws of admissible rotation matrices are used to approximate the bounds of the identified set. If after 10,000 draws of rotation matrices none of the draws satisfied the identification restrictions, the identified set is considered to be empty.

Figure 6: Responses to the ACITR shock.

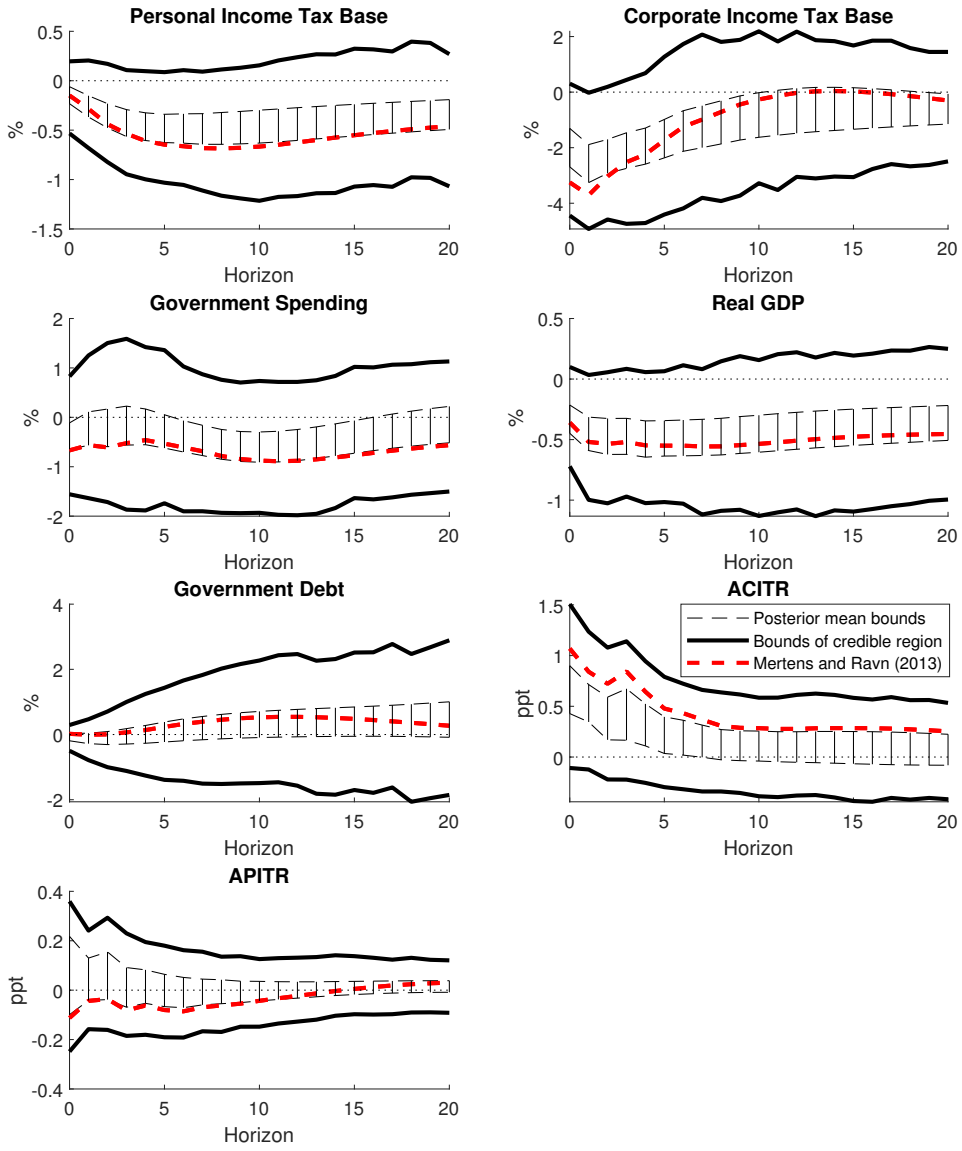

The results are based on 1,000 draws from the posterior of the reduced form coefficients and 1,000 draws of admissible rotation matrices are used to approximate the bounds of the identified set. If after 10,000 draws of rotation matrices none of the draws satisfied the identification restrictions, the identified set is considered to be empty.

Additionally, I impose that the correlation of the shock with its respective instrument is positive and each shock is more strongly correlated to its respective proxy than to the proxy for the other tax shock. These restrictions were also used by the robustness check in the work of Giacomini et al. (2021). However, different to their study I do not impose any sign restrictions of the impulse responses. The data spans the years 1950Q1 until 2006Q4 and are available in quarterly frequency. Like in the original study I estimate the VAR with four lags of the variables in the system and I employ the robust bayesian confidence bands for proxy VARs introduced by Giacomini et al. (2021). Doing so I follow their study and use independent Jeffreys' priors for the reduced form parameters of the proxy VAR.

Figure 5 and 6 depict the responses to the APITR and ACITR shock, respectively. In summary the results do not differ qualitatively substantially compared to the responses of the original study. Comparing the posterior means of the boundaries of the identified set (black dashed lines) and the results obtained with the identification strategy by Mertens and Ravn (2013) (red dashed lines) shows similar structural impulse responses. This is not surprising as the identification strategy employed in this robustness check is just a weaker version of the equality restrictions in Mertens and Ravn (2013). The weaker restrictions are reflected in less pronounced responses for many variables where the results of Mertens and Ravn (2013) are at or beyond the outer edge of the posterior mean bounds.

Looking at the robust bayesian credible regions reveal hardly any significant responses. This is consistent with the other findings by Jentsch and Lunsford (2019b) and Giacomini et al. (2021) who also fails to replicate the significant responses of Mertens and Ravn (2013) with more robust inference and/or less strict identification assumptions.

In conclusion this section provides evidence that this part of the results of Mertens and Ravn (2013) are qualitatively rather robust to weaker identification assumptions. Yet, they are statistically less convincing compared to the original study.

5.2 Empirical Illustration - Max-Share

This sections briefly describes a potential application for the combination of proxy VAR and Max-Share discussed above. The goal is to disentangle uncertainty shocks further into a portion that propagates through financial markets and a remaining part. Hence, the goal is to disentangle the uncertainty shock into two orthogonal 'sub-shocks'.

Financial frictions play a key role in the uncertainty literature for several reasons. Firstly, it is difficult to distinguish between financial frictions caused by uncertainty

Table 5: Propagation Mechanisms of Uncertainty

Contractionary	Ambiguous	Expansionary
Real options	Precautionary motives	Growth options
Risk premia		'Oi-Hartmann-Abel'

Different transmission channels described in the literature. See Bloom (2014) for a comprehensive overview.

and coming from other causes like e.g. changes in the banking sector or other systemic reasons. Both of the causes affect the economy similarly as the uncertainty shock at least partly consist of an financial market shock caused by it. Thus, it is hard to tell apart pure financial market shocks from uncertainty shocks and vice versa.

Second, financial frictions are viewed as a key transmission mechanisms of uncertainty on the real economy. Uncertainty is often further classified into financial, macroeconomic and policy uncertainty and the effects of the different types of uncertainty are studied separately. Similarly, to the financial market shocks it is difficult to tell apart the different types as uncertainty is also inherently hard to measure.

So far the literature concludes that uncertainty as well as financial market shocks have contractionary effects on the real economy (see e.g. Piffer & Podstawski, 2018; Bassett et al., 2014). Furthermore, studies that distinguish between financial uncertainty and macroeconomic/policy uncertainty tend to find more pronounced or exclusive effects for financial uncertainty (see e.g. Caldara et al., 2016; Alessandri & Mumtaz, 2019; Shin & Zhong, 2020). Yet, the identification strategies rely on measurements of the different uncertainty types, and therefore on the success of capturing them.

The approach I propose to disentangle how uncertainty affects the economy does not rely on the different types of uncertainty, but on the theoretical transmission channels identified by the literature. Under certain assumptions the proxy VAR framework together with the Max-Share approach can be employed to estimate the effects for different propagation mechanisms. Suppose two valid instruments for a common uncertainty shock are available. Then the combination of the two methods as described in section 2.4 is applicable. Assuming that the part of the uncertainty shock that propagates through financial markets maximizes the contribution to a key financial market variable, maximization problem (4) disentangles the two shocks. If the two instruments are solely related to the uncertainty shock other shocks are not considered in the maximization problem (as shown by the simulation in section 3.2) and the uncertainty shock is partitioned into two orthogonal components.

However, it is necessary to understand what the assumption implies. Table 8 lists

different transmission mechanisms identified by the literature. The contractionary ones are real option effects, which describe a 'wait and see' attitude that is implied by uncertainty, and increasing risk premia. According to empirical results these channels seem to dominate the remaining ones. Precautionary effects have ambivalent effects. On the one hand, precautionary savings have again contractionry effects, but on the other hand precautionary motives could also have expansionary effects. For example, economic agents could work more now in order to ensure for the uncertain future. Lastly, theory predicts also purely expansionary effects, yet, judging by the empirical results they are of minor importance. For a more comprehensive overview of the different transmission mechanisms see Bloom (2014).

One possibly interesting way to break up the uncertainty shock is to disentangle the effects of the risk premium channel from the rest, that is most likely dominated by the real option effects. Assuming the risk premium channel is the only channel propagating through financial markets on could identify the shock by maximizing the contribution to the FEV of a key financial market variable. Besides, one could also exploit the underlying recursive structure in this case and use the Cholesky decomposition.

Yet, if more than one transmission channel contributes to the FEV of the key financial market variable the results are potentially nevertheless interesting. The simulations show that in this case one identifies a combination of the these channels. In the example of an uncertainty shock one would identify a combination of all the channels propagating through the financial markets.

If, for example, two transmission channels propagates through the target variable, one identifies a combination of these two transmission channels as the first shock and again a mixture of the remaining ones as the second shock. In this case, the clear interpretation of a single transmission channel is not possible. What remains is the that the shock is broken up into two components and one of the components has the interpretation that it affects a specified variable exclusively. With the running example of the uncertainty shock, this would be the compound effect of all the channels that propagate through that variable.

Lastly, if all channels contribute to the FEV of the specified variable, one identifies the combination of all the different channels that maximizes the contribution. Now the other portion of the baseline shock has to the according orthogonal combination of the channels. Again, no clear interpretation regarding single channels is possible. One rather identifies the portion of the different channels that propagate through that one variable. In the running example, the portion that propagates through financial markets.

5.2.1 Disentangling Uncertainty with Proxies and Max-Share

To illustrate this strategy for the uncertainty shock I rely on the results of Piffer and Podstawski (2018). They identify an uncertainty shock using the variation of the gold price around exogenous events as an instrument. Furthermore, they identify a news shock as their instrument is also likely to be related to it. Assuming their identification strategy is successful I use their estimated median target shock as a purely exogenous instrument for a common uncertainty shock. In order to disentangle the uncertainty shocks in its 'sub-shocks' via the Max-Share approach I need a second proxy. As the second instrument I take two alternatives. Firstly, I regress their initial gold price instrument on the median target news shock and use the residual portion of the instrument as the second proxy. The idea is to purge the relation with news shocks, as e.g. done in a similar fashion by Bassett et al. (2014) Second, I use the median target shock in a single instrument proxy SVAR and use

Figure 7: Uncertainty Shock

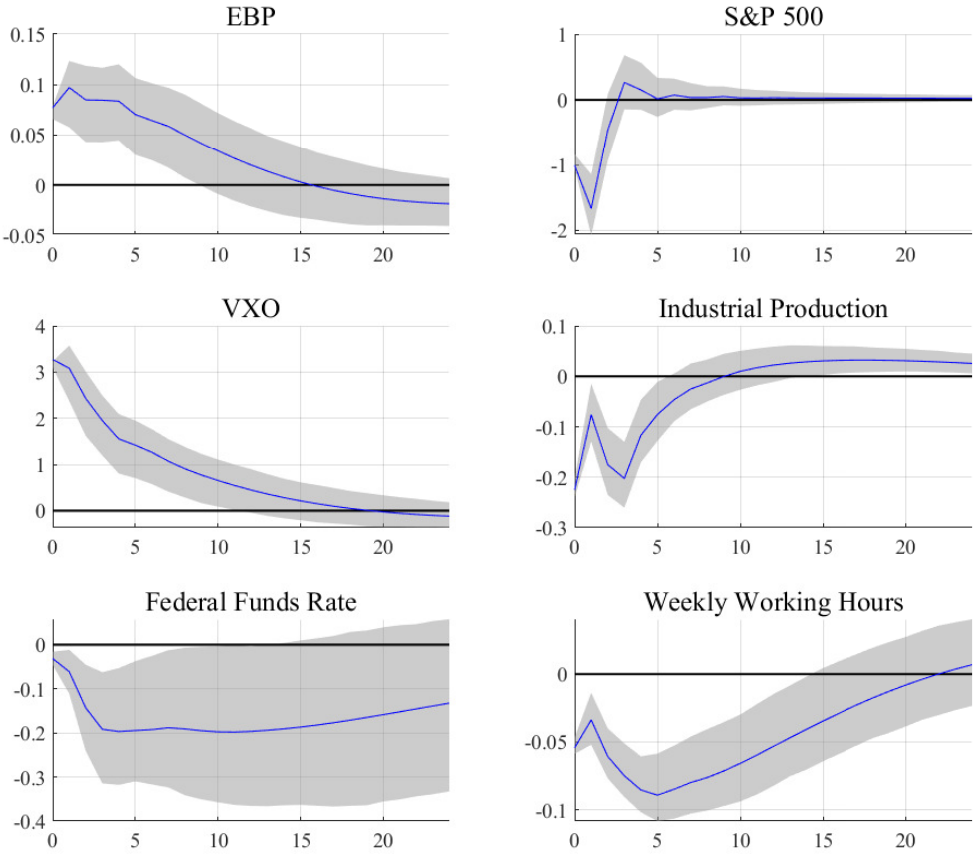

Structural impulse responses of an uncertainty shock identified with the median target shock of Piffer and Podstawski (2018) as a single instrument. Grey shaded areas depict the 95% wild bootstrap confidence bands.

the the resulting estimated shock as the second instrument.

I estimate a VAR model containing excess bond premium by Gilchrist and Zakrajšek (2012), log difference of the S&P 500, stock market volatility index VXO, log difference of industrial production, federal funds rate and the average weekly working hours. The shock is partitioned employing the maximization problem (4), in which I maximize the contribution to the excess bond premium. This credit spread measurement serves as the key financial market variable to single out the portion of the shock propagation financial markets. Restrictions on the relative correlation like in Piffer and Podstawski (2018) of the instruments with the uncertainty shock portions are not possible as it requires knowledge about which instrument is more strongly correlated to which shock portion.

Figure 5 shows the responses of an uncertainty shock identified using the median target uncertainty shock of Piffer and Podstawski (2018) as a single instrument. The grey shaded areas are the 95% wild bootstrap confidence bands. Higher uncertainty, depicted by the increase of the VXO, affects financial markets, output and also the labour market. Excess bond premium and the S&P 500 react as well as industrial production and the federal funds rate. Average weekly working hours decrease as

Figure 8: Partitioned Uncertainty Shock - Estimated Shock

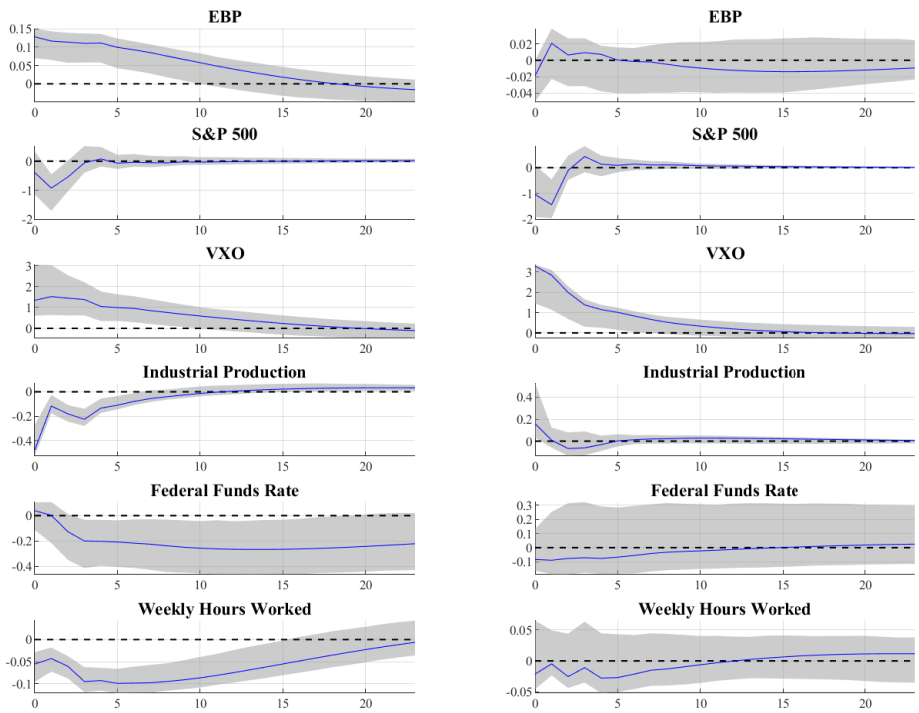

Structural impulse responses of the partitioned uncertainty shock. The two intruments are the median target shock of Piffer and Podstawski (2018) and the estimated shock behind Figure 5. Grey shaded areas depict the 95% wild bootstrap confidence bands.

a representative for the labour market side. For Figure 6, I use the median target shock of Piffer and Podstawski (2018) and the estimated shock behind Figure 5 as instruments for the multi-instrument application. For Figure 7 I use again the median target shock of Piffer and Podstawski (2018) and their cleaned gold price proxy. With the two estimated shocks as proxies (Figure 6) the identified portion of the shock contributes on average 43.24% to the FEV of the excess bond premium for $H = 13$ while the residual portion only contributes 0.61%. However, it is unclear whether the first shock depicts the effects of increasing risk premia alone or other transmission mechanism also affect the financial markets. When using the cleaned instrument, the identified portion contributes on average 87.82% and the residual portion 1.36%. This could indicate that the cleaned proxy is not purely exogenous and structural shocks other than the uncertainty shock are factored in, because it is unlikely that the uncertainty shock alone contributes roughly 90% to the FEV of the excess bond premium over the chosen horizon.

Figures 6 and 7 present the structural impulse responses for the partitioned uncertainty shock. Figure 6 show the results using the two estimated shocks as proxies and Figure 7 the responses using the cleaned instrument of Piffer and Podstawski

Figure 9: Partitioned Uncertainty Shock - Cleaned Instrument

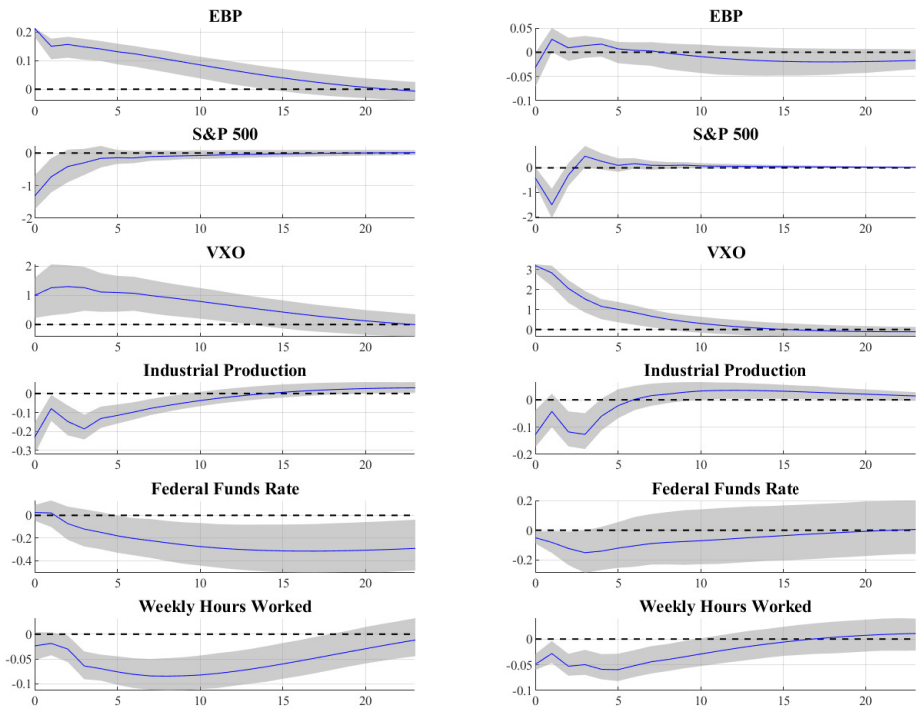

Structural impulse responses of the partitioned uncertainty shock. The two intruments are the median target shock of Piffer and Podstawski (2018) and their cleaned gold price proxy. Grey shaded areas depict the 95% wild bootstrap confidence bands.

(2018). In both figures the portion of the shock that maximizes the contribution to the excess bond premium is depicted on the left. Throughout both sets of responses it is visible that the contractionary effects on industrial production are more pronounced for the financial market portion of the the shock. In Figure 6 industrial production even exclusively reacts to this portion of the shock and has an initially expansionary tendency for the residual portion of the uncertainty shock. This is potentially surprising, yet, it could be explained, for example, by precautionary motives. Also the responses of the federal funds rate and working hours are more pronounced or exclusive. Only the S&P 500 and the VXO do not follow this pattern. Overall, the results are in line with previous results of the literature that suggest that financial frictions are the key propagation mechanisms of uncertainty shocks. However, the cleaned proxy is potentially prone to endogeneity issues.

5.2.2 Disentangling Uncertainty with Proxies and augmented Max-Share

To come.

6 Conclusion

Identifying restrictions on the FEV can be used in multiple ways to disentangle the shocks in the proxy VAR framework. Firstly, bounds the FEV as introduced by Volpicella (2021) replace or accompany other inequality restrictions to disentangle the shocks in the proxy VAR. This paper provides the general framework of the bounds applied to the proxy VAR, how to conduct robust bayesian inference in this setting and an empirical illustration that showcases a case where less restrictive bounds can be used to replace strict equality restrictions. In the empirical example I revisit the analysis of Mertens and Ravn (2013) and show that their results are overall less pronounced and less statistically convincing with less restrictive identification assumptions and robust inference.

Second, the structural parameters are sharply point identified in the proxy VAR with the help of the Max-Share framework. In the highly relevant case of two proxies the bias due to confounding shocks in Max-Share approach can be tackled. The simulation study shows that the proxies variables rule out confounding shocks which are not related to them. If confounding shocks are related to the proxies a correct inequality restriction on relative magnitudes of responses enables to get rid of the bias. Formalization of these findings and a suiting empirical illustration are prospect to further work. Lastly, the Max-Share approach augmented with the correct inequality restriction identifies the structural parameters more sharply than a set identification scheme based on the same inequality restrictions alone.

References

Alessandri, P., & Mumtaz, H. (2019). Financial regimes and uncertainty shocks. *Journal of Monetary Economics*, *101*, 31-46.

An, S., & Schorfheide, F. (2007). Bayesian Analysis of DSGE models. *Econometric Reviews*, *26*(2-4), 113-172.

Barsky, R. B., & Sims, E. R. (2011). News shocks and business cycles. *Journal of Monetary Economics*, *58*(3), 273-289.

Bassett, W. F., Chosak, M. B., Driscoll, J. C., & Zakrajšek, E. (2014). Changes in bank lending standards and the macroeconomy. *Journal of Monetary Economics*, *62*, 23-40.

Baumeister, C., & Hamilton, J. D. (2015). Sign restrictions, structural vector autoregressions, and useful prior information. *Econometrica*, *83*(5), 1963–1999.

Ben Zeev, N., & Pappa, E. (2017). Chronicle of a War Foretold: The Macroeconomic Effects of Anticipated Defence Spending Shocks. *The Economic Journal*, *127*(603), 1568-1597.

Bloom, N. (2014, May). Fluctuations in Uncertainty. *Journal of Economic Perspectives*, *28*(2), 153-76.

Brüggemann, R., Jentsch, C., & Trenkler, C. (2016). Inference in VARs with conditional heteroskedasticity of unknown form. *Journal of Econometrics*, *191*(1), 69-85.

Caldara, D., Fuentes-Albero, C., Gilchrist, S., & Zakrajšek, E. (2016). The macroeconomic impact of financial and uncertainty shocks. *European Economic Review*, *88*, 185-207. (SI: The Post-Crisis Slump)

Dieppe, A., Neville, F., & Kindberg-Hanlon, G. (2019). *New Approaches to the Identification of Low-Frequency Drivers: An Application to Technology Shocks*. The World Bank.

Faust, J. (1998). The robustness of identified VAR conclusions about money. *Carnegie-Rochester Conference Series on Public Policy*, *49*, 207-244.

Francis, N., Owyang, M. T., Roush, J. E., & DiCecio, R. (2014). A Flexible Finite-Horizon Alternative to Long-Run Restrictions with an Application to Technology Shocks. *The Review of Economics and Statistics*, *96*(4), 638-647.

Gertler, M., & Karadi, P. (2015, January). Monetary Policy Surprises, Credit Costs, and Economic Activity. *American Economic Journal: Macroeconomics*, *7*(1), 44-76.

Giacomini, R. (2013, 12). The relationship between DSGE and VAR models. In *Advances in econometrics* (Vol. 32, p. 1-25).

Giacomini, R., Kitagawa, T., & Read, M. (2021). Robust bayesian inference in proxy svars. *Journal of Econometrics*.

Gilchrist, S., & Zakrajšek, E. (2012, June). Credit Spreads and Business Cycle Fluctuations. *American Economic Review*, *102*(4), 1692-1720.

Jentsch, C., & Lunsford, K. G. (2019a, May). *Asymptotically Valid Bootstrap Inference for Proxy SVARs* (Working Papers No. 201908).

Jentsch, C., & Lunsford, K. G. (2019b, July). The dynamic effects of personal and corporate income tax changes in the united states: Comment. *American Economic Review*, *109*(7), 2655-78.

Kilian, L., & Lütkepohl, H. (2017). *Structural vector autoregressive analysis*. Cambridge University Press.

Komunjer, I., & Ng, S. (2011). Dynamic identification of dynamic stochastic general equilibrium models. *Econometrica*, *79*(6), 1995–2032.

Mertens, K., & Ravn, M. O. (2013, June). The Dynamic Effects of Personal and Corporate Income Tax Changes in the United States. *American Economic Review*, *103*(4), 1212-47.

Montiel Olea, J. L., & Nesbit, J. (2021). (machine) learning parameter regions. *Journal of Econometrics*, *222*(1, Part C), 716-744.

Piffer, M., & Podstawski, M. (2018). Identifying Uncertainty Shocks Using the Price of Gold. *The Economic Journal*, *128*(616), 3266-3284.

Romer, C. D., & Romer, D. H. (2010, June). The macroeconomic effects of tax changes: Estimates based on a new measure of fiscal shocks. *American Economic Review*, *100*(3), 763-801.

Shin, M., & Zhong, M. (2020). A new approach to identifying the real effects of uncertainty shocks. *Journal of Business & Economic Statistics*, *38*(2), 367-379.

Stock, J., & Watson, M. (2012). Disentangling the Channels of the 2007-2009 Recession. *Brookings Papers on Economic Activity*, *Spring 2012*, 81-135.

Uhlig, H. (2004a). Do technology shocks lead to a fall in total hours worked? *Journal of the European Economic Association*, *2*(2-3), 361-371.

Uhlig, H. (2004b). *What moves GNP?* (Econometric Society 2004 North American Winter Meetings No. 636).

Volpicella, A. (2021). Svars identification through bounds on the forecast error variance. *Journal of Business & Economic Statistics*, *0*(0), 1-11.

A Appendix A

Proof of Proposition 3.1.

The proof of Proposition 3.1 closely follows the ideas of the proof for Proposition 3.1 in the article by Volpicella (2021). The contribution of shock j to the FEV of variable i at horizon h is given by:

$$\Omega_{i,j}(h) = q_j' R_{i,h} q_j, \tag{32}$$

where $R_{i,h}$ is a positive semidefinite symmetric $l \times l$ real matrix. As $R_{i,h}$ is symmetric it can be diagonalized such that:

$$P' R_{i,h} P = D, \tag{33}$$

where P is an orthogonal matrix and D a diagonal matrix with the real eigenvalues λ_m^{ih} of matrix $R_{i,h}$ as entries on the diagonal for $m = 1, ..., l$.

For the $l \times 1$ orthogonal eigenvector q_m it holds that:

$$R_{i,h} q_m = \lambda_m^{ih} q_m, \tag{34}$$

and thus:

$$q_m' R_{i,h} q_m = \lambda_m^{ih} q_m' q_m = \lambda_m^{ih}. \tag{35}$$

The bound restrictions on the FEV are collected by:

$$\underline{\tau}_{i,j,h} \leq q_j' R_{i,h} q_j \leq \overline{\tau}_{i,j,h}, \text{ for } i \in \mathcal{I}_j \text{ and } h \in \mathcal{H}_{ij}. \tag{36}$$

Hence, if there exists an eigenvalue for which $\underline{\tau}_{i,j,h} \leq \lambda_m^{ih} \leq \overline{\tau}_{i,j,h}$ it holds that:

$$\underline{\tau}_{i,j,h} \leq q_m' R_{i,h} q_m \leq \overline{\tau}_{i,j,h}, \tag{37}$$

and condition (a) is satisfied for $q_j = q_m$. Condition (b) states that q_m satisfies also the remaining bound restrictions for all $i \in \mathcal{I}_j$ and $h \in \mathcal{H}_{ij}$ and the all the other identifying restrictions that are imposed. It follow that there exists an orthogonal matrix $Q = [q_1, ..., q_m, ..., q_l]$ for which all restrictions are satisfied and the identified set is non-empty.

Given that the identified set for the structural impulse responses is non-empty $\eta_{i,j,h} = e_i' C_m B_z q_j$ exists. Due to the restriction that the reduced-form VAR process is invertible in holds that $||e_i' C_m B_z|| < \infty$. Thus, it holds that $|\eta_{i,j,h}| \leq ||e_i' C_m B_z|| < \infty$ and the identified set for the impulse responses is bounded.

■

B Appendix B

Figure 10: 95% Point Estimate Bands, $\epsilon = 0.2$

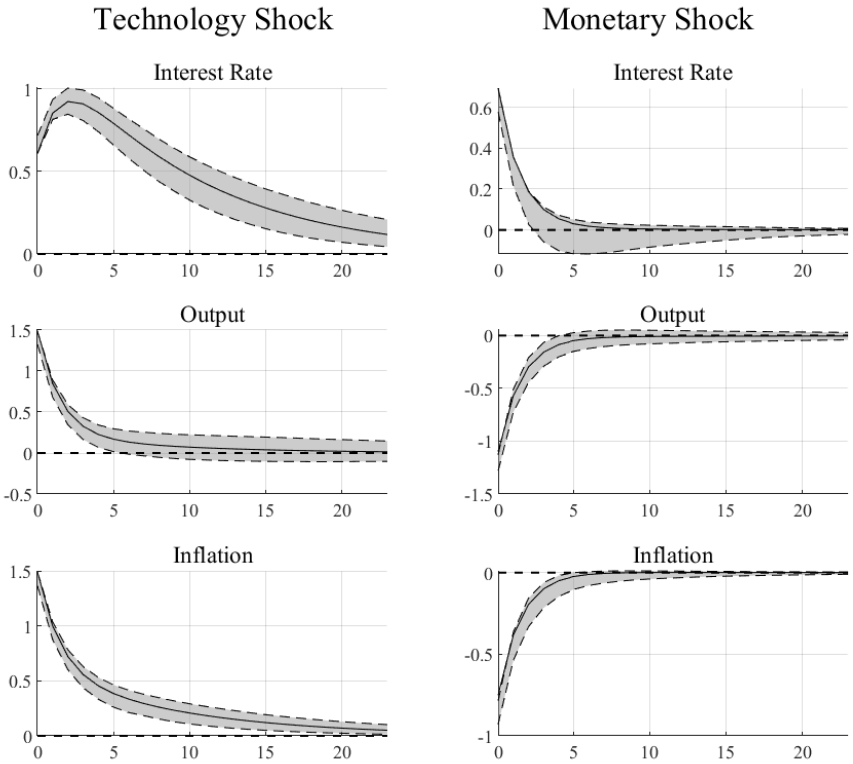

The solid lines are the true impulse responses and the dashed lines are the 2,5% and 97,5% quantile of the solutions found for the 1,000 simulation iterations.

Table 6: Bias of the IRFs to the Technology Shock, $T = 250$ - Scenario B

Variable	$H = 0$	$H = 6$	$H = 12$	$H = 18$
Panel A: $\epsilon = 0.38$				
r_t	0.0023	-0.0745	-0.0736	-0.0473
x_t	-0.0084	-0.0381	-0.0173	-0.0059
π_t	-0.0072	-0.0576	-0.0398	-0.0219
Panel B: $\epsilon = 0.2$				
r_t	0.0484	-0.0748	-0.0739	-0.0474
x_t	-0.0846	-0.0394	-0.0171	-0.0058
π_t	-0.0607	-0.059	-0.0399	-0.0219
Panel C: $\epsilon = 0$				
r_t	0.0956	-0.0795	-0.0764	-0.0485
x_t	-0.1803	-0.0421	-0.0176	-0.006
π_t	-0.1302	-0.0624	-0.0409	-0.0224

The table depicts the average of the estimated structural parameters over the 1,000 Monte-Carlo simulation iterations. The estimates are derived with the Max-Share$^+$ framework in the proxy VAR with different values of ϵ.

Table 7: Bias of the IRFs to the Monetary Shock, $T = 250$ - Scenario B

Variable	$H = 0$	$H = 6$	$H = 12$	$H = 18$
Panel A: $\epsilon = 0.38$				
r_t	-0.0026	-0.0105	-0.003	-0.0001
x_t	-0.0016	0.0032	0.0049	0.0039
π_t	-0.005	-0.0046	-0.0003	0.0004
Panel B: $\epsilon = 0.2$				
r_t	-0.0465	-0.0561	-0.0249	-0.011
x_t	-0.1053	-0.0041	0.0017	0.0021
π_t	-0.1082	-0.024	-0.0093	-0.0042
Panel C: $\epsilon = 0$				
r_t	-0.0986	-0.1052	-0.0486	-0.0228
x_t	-0.2086	-0.011	-0.0012	0.0005
π_t	-0.2146	-0.0449	-0.0189	-0.0092

The table depicts the average of the estimated structural parameters over the 1,000 Monte-Carlo simulation iterations. The estimates are derived with the Max-Share$^+$ framework in the proxy VAR with different values of ϵ.

Figure 11: Bias of the IRFs to the Technology Shock, $T = 250$ - Scenario B

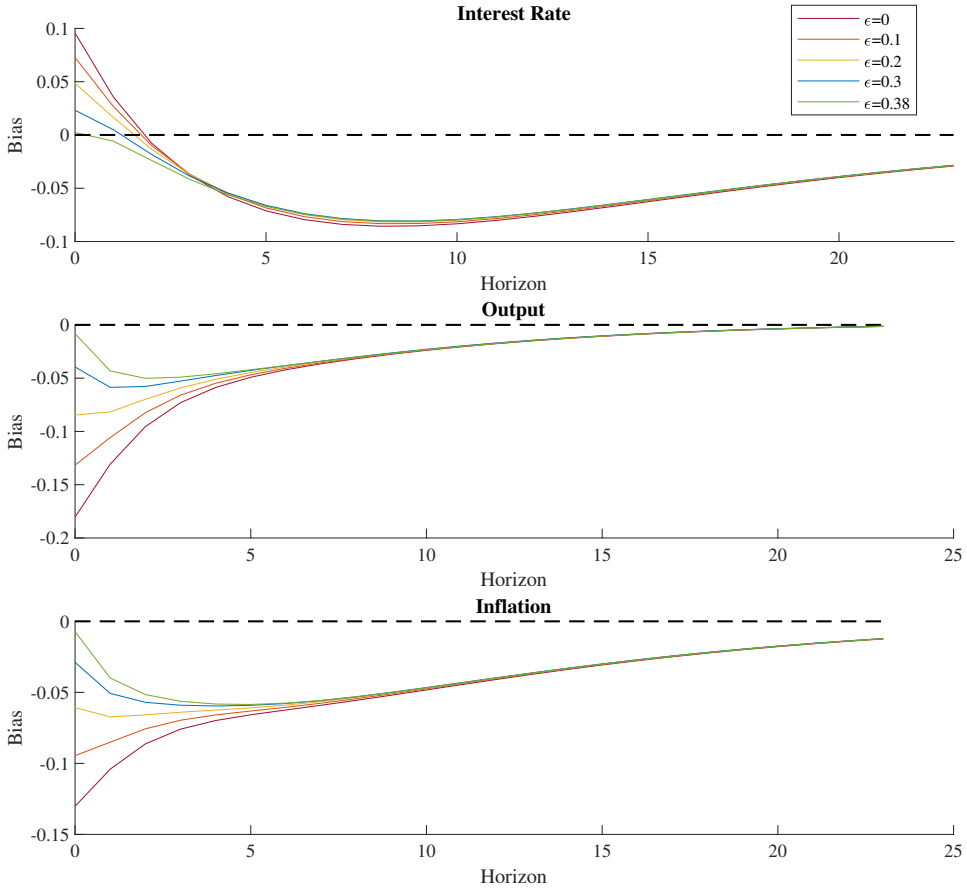

The coloured lines depict the average bias of the impulse response functions over 1,000 Monte-Carlo simulations for different values of ϵ.

Figure 12: Bias of the IRFs to the Monetary Shock, $T = 250$ - Scenario B

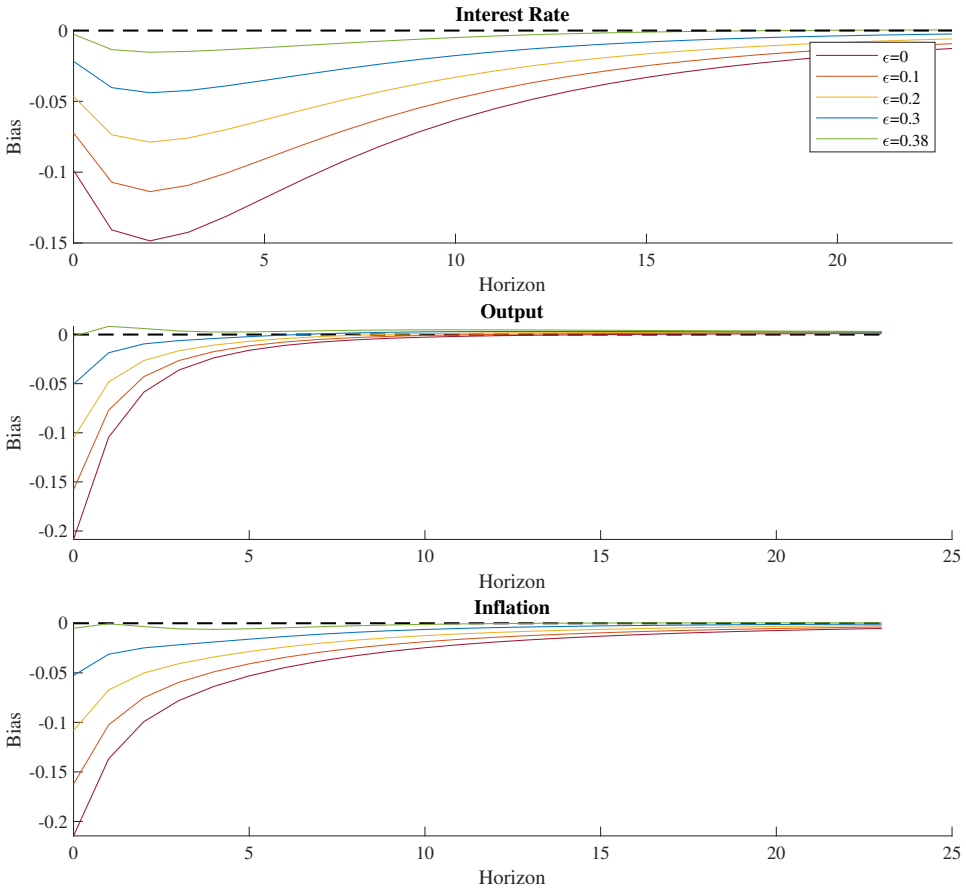

The coloured lines depict the average bias of the impulse response functions over 1,000 Monte-Carlo simulations for different values of ϵ.

Figure 13: Point Estimate Bands and Sign Restriction Sets, $\epsilon = 0$.

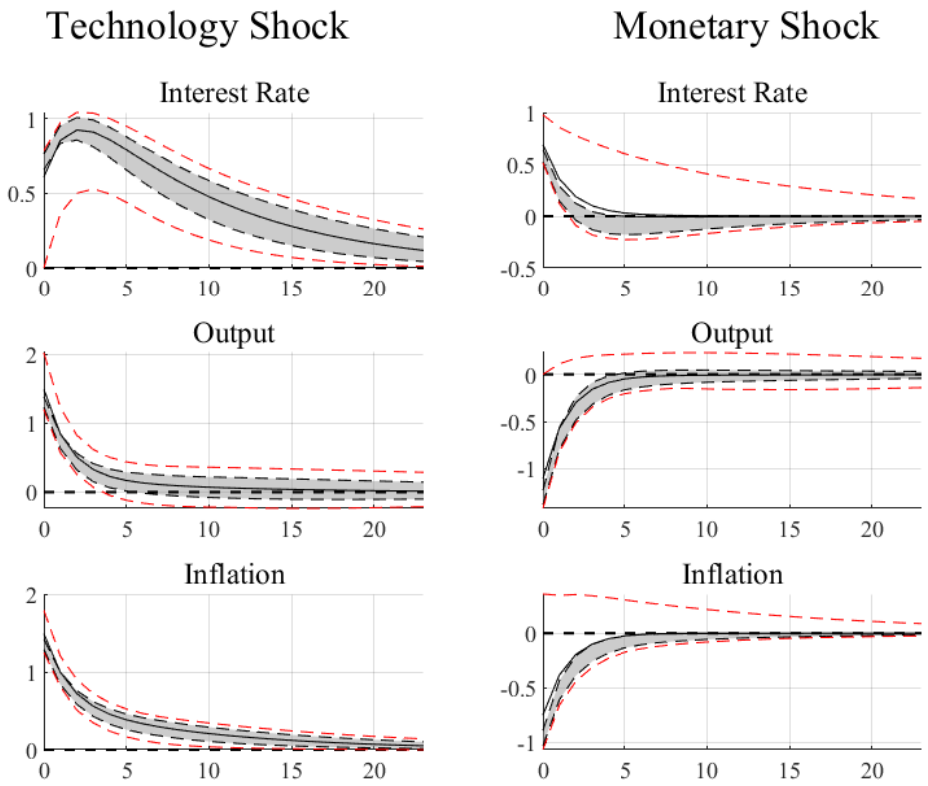

The solid lines are the true impulse responses and the dashed lines are the 2,5% and 97,5% quantile of the solutions found for the 1,000 simulation iterations. The red dashed line are the maximum and minimum responses of the identified set of the proxy SVAR disentangled via pure sign restrictions. The sign restrictions correspond to the constraints of the maximization problem.